

Alternatives to pyridinediimine ligands: syntheses and structures of metal complexes supported by donor-modified α -diimine ligands

Benjamin M. Schmiede,^a Michael J. Carney,^{*a} Brooke L. Small,^b Deidra L. Gerlach^a and Jason A. Halfen^a

Received 12th February 2007, Accepted 20th March 2007

First published as an Advance Article on the web 16th April 2007

DOI: 10.1039/b702197f

This report describes the synthesis and characterization of metal halide complexes (M = Mn, Fe, Co) supported by a new family of pendant donor-modified α -diimine ligands. The donor (N, O, P, S) substituent is linked to the α -diimine by a short hydrocarbon spacer forming a tridentate, *mer*-coordinating ligand structure. The tridentate ligands are assembled from monoimine precursors, the latter being synthesized by selective reaction with one carbonyl group of the α -dione. While attempts to separately isolate tridentate ligands in pure form were unsuccessful, metal complexes supported by the tridentate ligand are readily synthesized *in-situ*, by forming the ligand in the presence of the metal halide, resulting in a metal complex which subsequently crystallizes out of the reaction mixture. Metal complexes with NNN, NNO, NNP and NNS donor sets have been prepared and examples supported by NNN, NNP and NNS ligands have been structurally characterized. In the solid state, NNN and NNP ligands coordinate in a *mer* fashion and the metal complexes possess distorted square pyramidal structures and high spin (S = 2) electronic configurations. Compounds with NNS coordination environments display a variety of solid state structures, ranging from those with unbound sulfur atoms, including chloride bridged and solvent ligated species, to those with sulfur weakly bound to the metal center. The extent of sulfur ligation depends on the donor ability of the crystallization solvent and the substitution pattern of the arylthioether substituent.

Introduction

Over the past decade, ligands with imine functional groups have found wide use in olefin polymerization catalysis. For example, Brookhart demonstrated that nickel(II) and palladium(II) complexes supported by α -diimine ligands are effective α -olefin polymerization catalysts in the presence of methylalumoxane (MAO). Of particular note, nickel and palladium diimine catalysts polymerize ethylene to an unusual highly branched polyethylene (*via* a chain walking mechanism)¹ and palladium diimine catalysts are able to copolymerize α -olefins and functionalized vinyl monomers.² More recently, Gibson³ and Brookhart⁴ separately showed that iron(II) halides supported by pyridinebisimine (PBI) ligands display exceptional reactivity towards ethylene, producing α -olefin oligomers or high density polyethylene depending on the size and location of substituents on the imino-aryl rings. Since the initial reports by Gibson and Brookhart, which detailed the impact that imino-aryl substituents have on catalyst activity and product properties, more recent studies have examined the effect of heteroatom (*e.g.* Cl, Br, I⁵; F⁶; OMe, CF₃)⁷ substituted imino-aryl groups on iron(II)-PBI catalyst activity and oligomer properties. Of particular relevance was the ability to alter the product distribution from high molar mass polymers to low molar mass oligomers by varying the substitution pattern of the aryl ring.

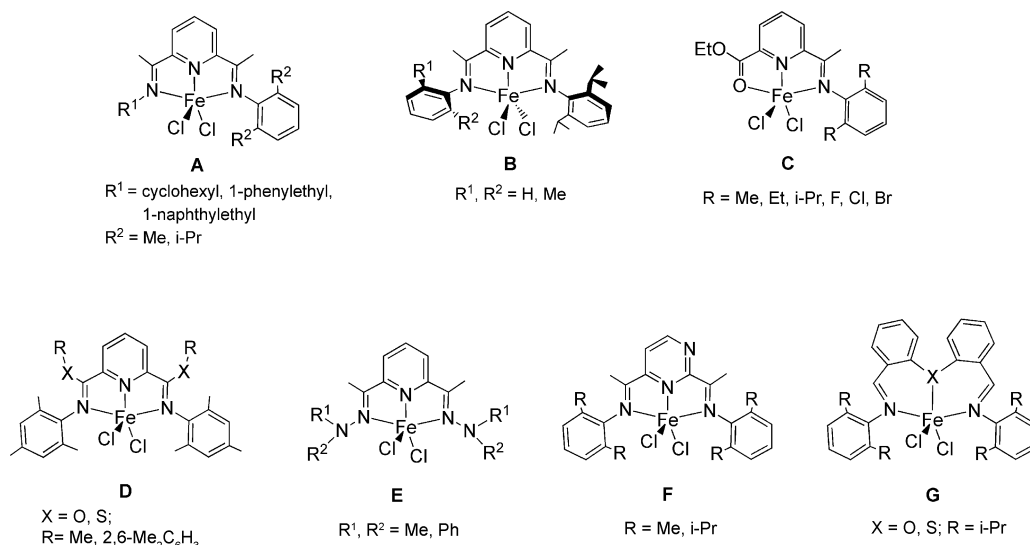
In addition, iron(II) complexes supported by asymmetric versions of PBI ligands have also been studied. These asymmetric

ligands are formed *via* sequential and selective reaction of bulky anilines with the α -dione carbonyl groups; examples of such ligands are shown as A–C^{8–10} in Scheme 1. Here the ability to modify the oligomer product distribution, as measured by the Schulz–Flory constant, *K*, has been well documented. In a rather dramatic case, the iron(II) catalyst with ligand B switches from producing oligomers to polyethylene by replacing the hydrogen 2,6-aryl substituents on one ring with methyl groups. Finally, PBI-related ligands, formed by placing heteroatoms in the ligand backbone, have also been explored. Selected examples are shown as ligands D–G in Scheme 1.^{11–13} Such ligand modifications often have a large impact on subsequent catalyst activity and oligomer properties, particularly on the Schulz–Flory constant. The ability to vary *K* over a fairly wide range, with, in most cases, relatively small changes in ligand structure, has fueled our interest in this area. Control over *K* is particularly important in an industrial setting where the ability to modify the product distribution *via* catalyst modification can provide α -olefin producers with another handle to optimize the value of the oligomeric product exiting the reactor.

We are especially interested in the use of alternative tridentate ligands that resemble the overall coordination geometry of PBI systems, but which allow for more substantial ligand (electronic and steric) variation. In particular, we wished to introduce alternative donors (O, P, S) into a tridentate ligand environment and we targeted strategies that allowed us to separately modify the donor heteroatom and its substituents. Moreover, since most PBI and α -diimine ligands reported to date are comprised of *aryl*imine functional groups, we also sought routes to more electronically diverse *alkyl*-substituted imines. This report outlines the syntheses and structures of divalent metal complexes supported by *mer*-ligating acenaphthene-diimine ligands, which have been modified

^aDepartment of Chemistry, University of Wisconsin-Eau Claire, 105 Garfield Avenue, Eau Claire, WI, USA 54702. E-mail: carneymj@uwec.edu; Fax: +1-715-836-4979; Tel: +1-715-836-3500

^bChevron Phillips Chemical Company, LP, 1862 Kingwood Drive, Kingwood, TX, 77339, USA



Scheme 1

with an additional pendant donor (N, O, P, S) atom. The metal complexes described herein are supported by unique asymmetric, donor-modified acenaphthene-diimine ligands incorporating stable *n*-alkylimine functional groups.

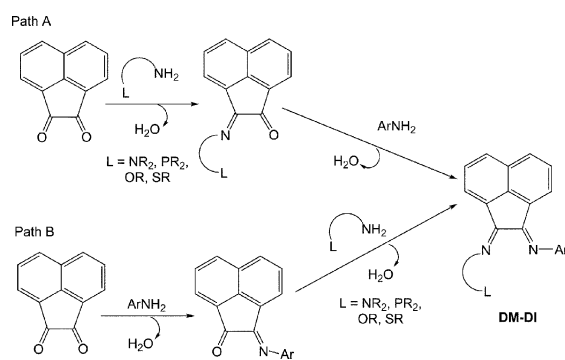
Results and discussion

Preparation of monoimine ligand precursors

We set out to prepare *mer*-ligating tridentate ligands comprised of a donor-modified α -diimine (DM-DI in Scheme 2). Such ligands would provide the desired *mer*-coordination geometry, but would allow for extensive ligand variation by modifying the appended donor atom and its substituents. In contrast to the more symmetrical PBI donor atom arrangement, wherein the imine nitrogens flank a central pyridine ring, the DM-DI ligand positions the imines side-by-side with the pendant donor atom off to one side. Thus, ligands with various heteroatom donors and donor substituents, and with donors attached to the α -diimine by linking groups of various lengths, are accessible with the appropriate synthetic schemes. The ability to manipulate the ligand structure in a controlled fashion allows us to explore the impact of such ligand variations on metal complex structure and catalytic performance.

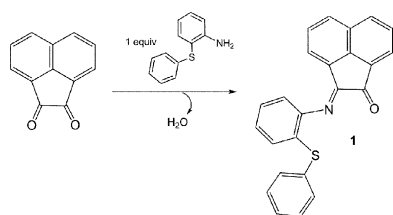
For our targeted asymmetric ligands, the appropriate synthetic schemes require the introduction of imine functional groups by selective reaction of one carbonyl group of the α -dione at a time. A recent report outlines a preparative scheme to synthesize asymmetric α -diimines,¹⁴ however no examples of ligands with pendant donor atoms were described. Similar synthetic schemes have been used to prepare the asymmetric PBI ligands mentioned previously (ligands A–C in Scheme 1).¹⁵

In the present case, two possible synthetic approaches were envisioned starting with acenaphthenequinone, these approaches are outlined in Scheme 2. The first (Path A) involves selective reaction of one carbonyl group with a donor-modified amine, followed by reaction of the remaining carbonyl with a bulky aniline derivative. The second route (Path B) reverses the order of addition of the bulky aniline derivative and the donor-modified amine. For



Scheme 2

Path A, successful formation of the donor-modified monoimine would seemingly favor subsequent derivatization (using a bulky aniline) at the more accessible carbonyl rather than at the just-introduced imine functionality. Unfortunately, attempts to prepare the initial donor-modified monoimines by reaction of acenaphthenequinone with one equivalent of a pendant donor-modified primary alkyl amine, such as 2-(aminomethyl)pyridine, 2-(aminoethyl)pyridine or *N,N*-dimethylethylenediamine did not yield isolable material. Instead a complex product mixture resulted.¹⁶ Analysis of the mixture by ¹H NMR suggested that, among other products, both diimine and monoimine products were formed, even when reaction conditions were employed to favor mono-substitution (*e.g.* slow addition of one equivalent of the amine to acenaphthenequinone). In one instance, reaction of acenaphthenequinone with one equivalent of the more sterically encumbered (and less basic) 2-phenylthioaniline did lead to selective monoimine formation (Scheme 3, compound 1). The isolated yellow powder displayed a complex solution ¹H NMR spectrum at room temperature, perhaps due to the presence of conformational isomers that interconvert slowly relative to the NMR timescale. Elemental analysis, GC-MS data and an X-ray crystal structure determination confirmed the monoimine formulation. The molecular geometry of 1 is shown in Fig. 1. Selected interatomic distances are listed in Table 2. The structure



Scheme 3

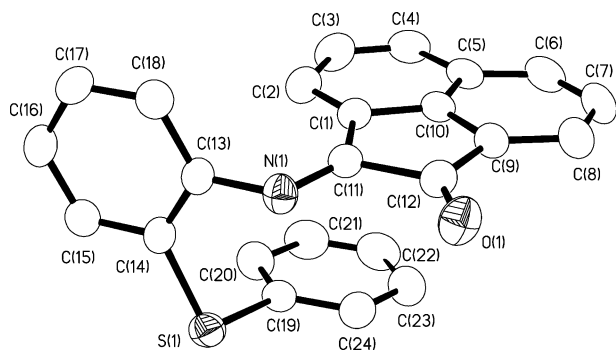
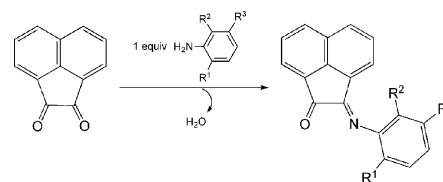


Fig. 1 Thermal ellipsoid representation (35% probability boundaries) of the X-ray crystal structure of monoimine **1** with hydrogen atoms omitted for clarity.

of **1** shows normal C=N (1.272(3) Å) and C=O (1.209(3) Å) bond lengths and is clearly consistent with the monoimine formulation. The structure also shows the thioether aryl substituent nestled underneath the acenaphthene ring in a coplanar arrangement (centroid to centroid distance = 3.66 Å), suggesting some level of π -stacking interactions between the two aromatic systems.



Scheme 4

Table 1 Summary of X-ray crystallographic data for monoimine **1** and NNN- and NNP-ligated metal complexes^a

Complex	1	(3a)FeCl ₂	(2c)FeCl ₂ ·0.5MeCN	(2d)FeCl ₂	(2a)MnCl ₂	(3g)FeCl ₂
Empirical formula	C ₂₄ H ₁₅ NOS	C ₂₈ H ₃₃ Cl ₂ FeN ₃	C ₂₈ H _{24.50} Cl ₂ FeN _{3.50}	C ₂₆ H ₂₇ Cl ₂ FeN ₃ O	C ₂₄ H ₂₅ Cl ₂ MnN ₃	C ₄₂ H ₄₃ Cl ₂ FeN ₄ P
FW	365.43	538.32	536.76	524.26	481.31	761.52
Crystal system	Orthorhombic	Orthorhombic	Triclinic	Triclinic	Monoclinic	Orthorhombic
Space group	<i>Pbca</i>	<i>P2₁2₁2₁</i>	<i>P</i> $\bar{1}$	<i>P</i> $\bar{1}$	<i>C2/c</i>	<i>Pna2₁</i>
<i>a</i> /Å	14.488(2)	9.336(2)	11.348(2)	12.309(1)	19.107(2)	10.690(2)
<i>b</i> /Å	15.586(2)	12.5150(8)	15.047(3)	14.355(3)	16.5813(7)	30.399(6)
<i>c</i> /Å	16.105(1)	23.120(3)	16.062(3)	14.553(2)	14.816(1)	11.998(2)
α /°	90	90	85.13(5)	89.42(2)	90	90
β /°	90	90	77.34(4)	77.51(1)	102.74(1)	90
γ /°	90	90	76.89(6)	77.48(1)	90	90
<i>V</i> /Å ³	3636.6(7)	2701.3(7)	2604.3(8)	2449.1(6)	4578.4(6)	3898.9(12)
<i>Z</i>	8	4	4	4	8	4
<i>d</i> _{calc} /Mg m ⁻³	1.335	1.324	1.369	1.422	1.397	1.297
Crystal size/mm	0.26 × 0.24 × 0.24	0.40 × 0.38 × 0.18	0.42 × 0.26 × 0.26	0.48 × 0.08 × 0.06	0.38 × 0.36 × 0.20	0.48 × 0.16 × 0.14
Abs. Coeff./mm ⁻¹	0.191	0.777	0.807	0.858	0.826	0.600
2 θ max/°	49.94	55.00	49.98	49.90	53.94	49.98
Transmission range	1.0–1.0	0.8728–0.7463	1.0–1.0	1.0–0.692	1.0–0.9514	0.995–0.839
No. of reflns collected	6225	6489	9637	8980	5125	7128
No. of indep reflns	3195	5874	9134	8545	4975	3609
No. of obsd reflections	1887	4548	6314	5260	4244	2575
No. of variables	244	313	623	599	275	453
<i>R</i> 1 (<i>wR</i> 2) ^b [<i>I</i> > 2 σ (<i>I</i>)]	0.0473 (0.0863)	0.0440 (0.0853)	0.0552 (0.1322)	0.0680 (0.1460)	0.0312 (0.0761)	0.0503 (0.0930)
Goodness-of-fit (<i>F</i> ²)	0.990	1.017	1.019	1.004	1.039	1.018
Diff. Peaks/e ⁻ Å ⁻³	0.153, -0.174	0.251, -0.275	0.645, -0.597	0.693, -0.618	0.246, -0.287	0.592, -0.452

^a See Experimental section for additional data collection, reduction, and structure solution and refinement details. ^b $R1 = \sum |F_o| - |F_c| / \sum |F_o|$; $wR2 = [\sum [w(F_o^2 - F_c^2)^2]]^{1/2}$ where $w = 1/\sigma^2(F_o^2) + (aP)^2 + bP$.

Table 2 Selected distances (Å) and angles (°) for monoimine **1** and NNN- and NNP-ligated metal complexes

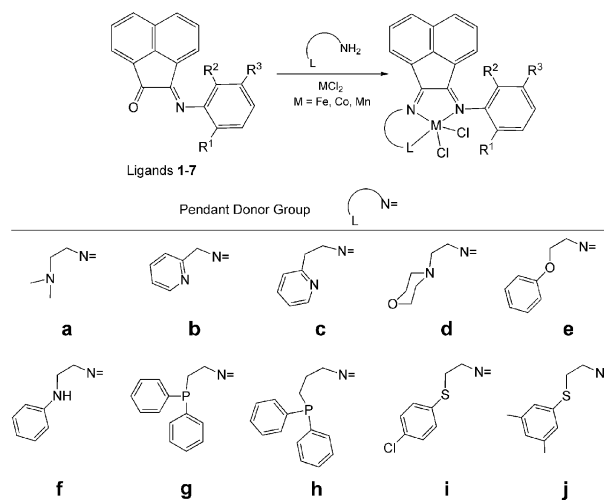
1	(3a)FeCl ₂		(2c)FeCl ₂		Molecule 2		(2d)FeCl ₂		Molecule 2		(2a)MnCl ₂		(3g)FeCl ₂		
	S(1)–C(14)	1.779(3)	Fe(1)–N(1)	2.137(3)	2.139(3)	Fe(2)–N(4)	2.102(4)	N(1)–Fe(1)–N(2)	73.92(17)	N(4)–Fe(2)–N(5)	73.92(17)	Mn(1)–N(1)	2.219(14)	Fe(1)–N(1)	2.181(6)
S(1)–C(19)	1.784(3)	2.195(3)	Fe(1)–N(2)	2.271(4)	2.271(4)	Fe(2)–N(5)	2.270(5)	Fe(1)–N(3)	77.25(17)	Fe(2)–N(6)	2.410(6)	Mn(1)–N(2)	2.3965(14)	Fe(1)–N(2)	2.166(6)
N(1)–C(11)	1.272(3)	2.164(3)	Fe(1)–N(3)	2.215(4)	2.215(4)	Fe(2)–N(6)	2.358(5)	Fe(1)–N(3)	75.56(17)	N(4)–Fe(2)–N(6)	78.74(17)	Mn(1)–N(3)	2.3099(14)	Fe(1)–N(3)	2.497(2)
N(1)–C(13)	1.421(3)	2.3153(11)	Fe(1)–Cl(1)	2.3308(16)	2.3308(16)	Fe(2)–Cl(3) <td>2.307(2)</td> <th>Fe(1)–Cl(1) <td>103.21(14)</td> <th>N(4)–Fe(2)–Cl(3) <td>126.75(15)</td> <th>Mn(1)–Cl(1)</th> <td>2.3495(5)</td> <th>Fe(1)–Cl(1) <td>2.287(2)</td> </th></th></th>	2.307(2)	Fe(1)–Cl(1) <td>103.21(14)</td> <th>N(4)–Fe(2)–Cl(3) <td>126.75(15)</td> <th>Mn(1)–Cl(1)</th> <td>2.3495(5)</td> <th>Fe(1)–Cl(1) <td>2.287(2)</td> </th></th>	103.21(14)	N(4)–Fe(2)–Cl(3) <td>126.75(15)</td> <th>Mn(1)–Cl(1)</th> <td>2.3495(5)</td> <th>Fe(1)–Cl(1) <td>2.287(2)</td> </th>	126.75(15)	Mn(1)–Cl(1)	2.3495(5)	Fe(1)–Cl(1) <td>2.287(2)</td>	2.287(2)
O(1)–C(12)	1.209(3)	2.2821(10)	Fe(1)–Cl(2)	2.2952(17)	2.2952(17)	Fe(2)–Cl(4) <td>2.3228(16)</td> <th>Fe(1)–Cl(2) <td>137.57(14)</td> <th>N(4)–Fe(2)–Cl(4) <td>109.67(15)</td> <th>Mn(1)–Cl(2)</th> <td>2.3524(5)</td> <th>Fe(1)–Cl(2)</th> <td>2.3131(18)</td> </th></th>	2.3228(16)	Fe(1)–Cl(2) <td>137.57(14)</td> <th>N(4)–Fe(2)–Cl(4) <td>109.67(15)</td> <th>Mn(1)–Cl(2)</th> <td>2.3524(5)</td> <th>Fe(1)–Cl(2)</th> <td>2.3131(18)</td> </th>	137.57(14)	N(4)–Fe(2)–Cl(4) <td>109.67(15)</td> <th>Mn(1)–Cl(2)</th> <td>2.3524(5)</td> <th>Fe(1)–Cl(2)</th> <td>2.3131(18)</td>	109.67(15)	Mn(1)–Cl(2)	2.3524(5)	Fe(1)–Cl(2)	2.3131(18)
C(11)–C(12)	1.545(4)	1.268(4)	N(1)–C(11)	1.289(5)	1.289(5)	N(4)–C(40) <td>1.269(5)</td> <th>N(1)–C(11) <td>95.84(13)</td> <th>N(4)–C(37) <td>1.266(7)</td> <th>N(1)–C(11)</th> <td>1.272(2)</td> <th>Fe(1)–C(11)</th> <td>1.304(9)</td> </th></th>	1.269(5)	N(1)–C(11) <td>95.84(13)</td> <th>N(4)–C(37) <td>1.266(7)</td> <th>N(1)–C(11)</th> <td>1.272(2)</td> <th>Fe(1)–C(11)</th> <td>1.304(9)</td> </th>	95.84(13)	N(4)–C(37) <td>1.266(7)</td> <th>N(1)–C(11)</th> <td>1.272(2)</td> <th>Fe(1)–C(11)</th> <td>1.304(9)</td>	1.266(7)	N(1)–C(11)	1.272(2)	Fe(1)–C(11)	1.304(9)
		1.302(4)	N(2)–C(12)	1.286(5)	1.286(5)	N(5)–C(41) <td>1.281(5)</td> <th>N(2)–C(12) <td>103.79(12)</td> <th>N(5)–C(38) <td>1.269(7)</td> <th>N(2)–C(12)</th> <td>1.281(2)</td> <th>Fe(1)–C(12)</th> <td>1.278(9)</td> </th></th>	1.281(5)	N(2)–C(12) <td>103.79(12)</td> <th>N(5)–C(38) <td>1.269(7)</td> <th>N(2)–C(12)</th> <td>1.281(2)</td> <th>Fe(1)–C(12)</th> <td>1.278(9)</td> </th>	103.79(12)	N(5)–C(38) <td>1.269(7)</td> <th>N(2)–C(12)</th> <td>1.281(2)</td> <th>Fe(1)–C(12)</th> <td>1.278(9)</td>	1.269(7)	N(2)–C(12)	1.281(2)	Fe(1)–C(12)	1.278(9)
C(14)–S(1)–C(19)	102.07(12)	74.95(10)	N(1)–Fe(1)–N(2)	75.51(12)	75.51(12)	N(4)–Fe(2)–N(5) <td>75.46(13)</td> <th>N(1)–Fe(1)–N(2) <td>77.25(17)</td> <th>N(4)–Fe(2)–N(5) <td>75.46(13)</td> <th>N(1)–Mn(1)–N(2)</th> <td>72.02(5)</td> <th>N(1)–Fe(1)–N(2)</th> <td>75.9(2)</td> </th></th>	75.46(13)	N(1)–Fe(1)–N(2) <td>77.25(17)</td> <th>N(4)–Fe(2)–N(5) <td>75.46(13)</td> <th>N(1)–Mn(1)–N(2)</th> <td>72.02(5)</td> <th>N(1)–Fe(1)–N(2)</th> <td>75.9(2)</td> </th>	77.25(17)	N(4)–Fe(2)–N(5) <td>75.46(13)</td> <th>N(1)–Mn(1)–N(2)</th> <td>72.02(5)</td> <th>N(1)–Fe(1)–N(2)</th> <td>75.9(2)</td>	75.46(13)	N(1)–Mn(1)–N(2)	72.02(5)	N(1)–Fe(1)–N(2)	75.9(2)
C(11)–N(1)–C(13)	119.5(2)	75.53(9)	N(1)–Fe(1)–N(3)	85.27(13)	85.27(13)	N(4)–Fe(2)–N(6) <td>82.76(13)</td> <th>N(1)–Fe(1)–N(3) <td>77.25(17)</td> <th>N(4)–Fe(2)–N(6) <td>82.76(13)</td> <th>N(1)–Mn(1)–N(3)</th> <td>72.87(5)</td> <th>N(1)–Fe(1)–N(3)</th> <td>74.01(16)</td> </th></th>	82.76(13)	N(1)–Fe(1)–N(3) <td>77.25(17)</td> <th>N(4)–Fe(2)–N(6) <td>82.76(13)</td> <th>N(1)–Mn(1)–N(3)</th> <td>72.87(5)</td> <th>N(1)–Fe(1)–N(3)</th> <td>74.01(16)</td> </th>	77.25(17)	N(4)–Fe(2)–N(6) <td>82.76(13)</td> <th>N(1)–Mn(1)–N(3)</th> <td>72.87(5)</td> <th>N(1)–Fe(1)–N(3)</th> <td>74.01(16)</td>	82.76(13)	N(1)–Mn(1)–N(3)	72.87(5)	N(1)–Fe(1)–N(3)	74.01(16)
N(1)–C(11)–C(12)	119.9(2)	138.49(10)	N(2)–Fe(1)–N(3)	149.14(14)	149.14(14)	N(5)–Fe(2)–N(6) <td>143.57(5)</td> <th>N(2)–Fe(1)–N(3) <td>152.68(16)</td> <th>N(5)–Fe(2)–N(6) <td>152.54(17)</td> <th>N(2)–Mn(1)–N(3)</th> <td>139.43(5)</td> <th>N(2)–Fe(1)–N(3)</th> <td>135.20(16)</td> </th></th>	143.57(5)	N(2)–Fe(1)–N(3) <td>152.68(16)</td> <th>N(5)–Fe(2)–N(6) <td>152.54(17)</td> <th>N(2)–Mn(1)–N(3)</th> <td>139.43(5)</td> <th>N(2)–Fe(1)–N(3)</th> <td>135.20(16)</td> </th>	152.68(16)	N(5)–Fe(2)–N(6) <td>152.54(17)</td> <th>N(2)–Mn(1)–N(3)</th> <td>139.43(5)</td> <th>N(2)–Fe(1)–N(3)</th> <td>135.20(16)</td>	152.54(17)	N(2)–Mn(1)–N(3)	139.43(5)	N(2)–Fe(1)–N(3)	135.20(16)
N(1)–C(11)–C(1)	133.5(2)	96.43(8)	N(1)–Fe(1)–Cl(1)	99.41(10)	99.41(10)	N(4)–Fe(2)–Cl(3) <td>98.54(12)</td> <th>N(1)–Fe(1)–Cl(1) <td>103.21(14)</td> <th>N(4)–Fe(2)–Cl(3) <td>126.75(15)</td> <th>N(1)–Mn(1)–Cl(1)</th> <td>138.22(4)</td> <th>N(1)–Fe(1)–Cl(1)</th> <td>156.17(16)</td> </th></th>	98.54(12)	N(1)–Fe(1)–Cl(1) <td>103.21(14)</td> <th>N(4)–Fe(2)–Cl(3) <td>126.75(15)</td> <th>N(1)–Mn(1)–Cl(1)</th> <td>138.22(4)</td> <th>N(1)–Fe(1)–Cl(1)</th> <td>156.17(16)</td> </th>	103.21(14)	N(4)–Fe(2)–Cl(3) <td>126.75(15)</td> <th>N(1)–Mn(1)–Cl(1)</th> <td>138.22(4)</td> <th>N(1)–Fe(1)–Cl(1)</th> <td>156.17(16)</td>	126.75(15)	N(1)–Mn(1)–Cl(1)	138.22(4)	N(1)–Fe(1)–Cl(1)	156.17(16)
O(1)–C(12)–C(11)	124.3(2)	157.62(8)	N(1)–Fe(1)–Cl(2)	147.37(10)	147.37(10)	N(4)–Fe(2)–Cl(4) <td>154.42(11)</td> <th>N(1)–Fe(1)–Cl(2) <td>137.57(14)</td> <th>N(4)–Fe(2)–Cl(4) <td>109.67(15)</td> <th>N(1)–Mn(1)–Cl(2)</th> <td>109.09(4)</td> <th>N(1)–Fe(1)–Cl(2)</th> <td>91.85(16)</td> </th></th>	154.42(11)	N(1)–Fe(1)–Cl(2) <td>137.57(14)</td> <th>N(4)–Fe(2)–Cl(4) <td>109.67(15)</td> <th>N(1)–Mn(1)–Cl(2)</th> <td>109.09(4)</td> <th>N(1)–Fe(1)–Cl(2)</th> <td>91.85(16)</td> </th>	137.57(14)	N(4)–Fe(2)–Cl(4) <td>109.67(15)</td> <th>N(1)–Mn(1)–Cl(2)</th> <td>109.09(4)</td> <th>N(1)–Fe(1)–Cl(2)</th> <td>91.85(16)</td>	109.67(15)	N(1)–Mn(1)–Cl(2)	109.09(4)	N(1)–Fe(1)–Cl(2)	91.85(16)
O(1)–C(12)–C(9)	129.8(3)	101.26(8)	N(2)–Fe(1)–Cl(1)	105.16(12)	105.16(12)	N(5)–Fe(2)–Cl(3) <td>104.66(6)</td> <th>N(2)–Fe(1)–Cl(1) <td>95.84(13)</td> <th>N(5)–Fe(2)–Cl(3) <td>96.77(13)</td> <th>N(2)–Mn(1)–Cl(1)</th> <td>98.32(4)</td> <th>N(2)–Fe(1)–Cl(1)</th> <td>93.68(16)</td> </th></th>	104.66(6)	N(2)–Fe(1)–Cl(1) <td>95.84(13)</td> <th>N(5)–Fe(2)–Cl(3) <td>96.77(13)</td> <th>N(2)–Mn(1)–Cl(1)</th> <td>98.32(4)</td> <th>N(2)–Fe(1)–Cl(1)</th> <td>93.68(16)</td> </th>	95.84(13)	N(5)–Fe(2)–Cl(3) <td>96.77(13)</td> <th>N(2)–Mn(1)–Cl(1)</th> <td>98.32(4)</td> <th>N(2)–Fe(1)–Cl(1)</th> <td>93.68(16)</td>	96.77(13)	N(2)–Mn(1)–Cl(1)	98.32(4)	N(2)–Fe(1)–Cl(1)	93.68(16)
		100.20(8)	N(2)–Fe(1)–Cl(2)	88.12(11)	88.12(11)	N(5)–Fe(2)–Cl(4) <td>92.27(10)</td> <th>N(2)–Fe(1)–Cl(2) <td>94.56(13)</td> <th>N(5)–Fe(2)–Cl(4) <td>91.49(12)</td> <th>N(2)–Mn(1)–Cl(2)</th> <td>102.74(4)</td> <th>N(2)–Fe(1)–Cl(2)</th> <td>114.34(15)</td> </th></th>	92.27(10)	N(2)–Fe(1)–Cl(2) <td>94.56(13)</td> <th>N(5)–Fe(2)–Cl(4) <td>91.49(12)</td> <th>N(2)–Mn(1)–Cl(2)</th> <td>102.74(4)</td> <th>N(2)–Fe(1)–Cl(2)</th> <td>114.34(15)</td> </th>	94.56(13)	N(5)–Fe(2)–Cl(4) <td>91.49(12)</td> <th>N(2)–Mn(1)–Cl(2)</th> <td>102.74(4)</td> <th>N(2)–Fe(1)–Cl(2)</th> <td>114.34(15)</td>	91.49(12)	N(2)–Mn(1)–Cl(2)	102.74(4)	N(2)–Fe(1)–Cl(2)	114.34(15)
		110.48(7)	N(3)–Fe(1)–Cl(1)	101.59(12)	101.59(12)	N(6)–Fe(2)–Cl(3) <td>107.21(11)</td> <th>N(3)–Fe(1)–Cl(1) <td>92.81(13)</td> <th>N(6)–Fe(2)–Cl(3) <td>97.56(14)</td> <th>N(3)–Mn(1)–Cl(1)</th> <td>94.43(4)</td> <th>P(1)–Fe(1)–Cl(1)</th> <td>100.76(7)</td> </th></th>	107.21(11)	N(3)–Fe(1)–Cl(1) <td>92.81(13)</td> <th>N(6)–Fe(2)–Cl(3) <td>97.56(14)</td> <th>N(3)–Mn(1)–Cl(1)</th> <td>94.43(4)</td> <th>P(1)–Fe(1)–Cl(1)</th> <td>100.76(7)</td> </th>	92.81(13)	N(6)–Fe(2)–Cl(3) <td>97.56(14)</td> <th>N(3)–Mn(1)–Cl(1)</th> <td>94.43(4)</td> <th>P(1)–Fe(1)–Cl(1)</th> <td>100.76(7)</td>	97.56(14)	N(3)–Mn(1)–Cl(1)	94.43(4)	P(1)–Fe(1)–Cl(1)	100.76(7)
		110.48(7)	N(3)–Fe(1)–Cl(2)	95.85(12)	95.85(12)	N(6)–Fe(2)–Cl(4) <td>95.28(10)</td> <th>N(3)–Fe(1)–Cl(2) <td>103.79(12)</td> <th>N(6)–Fe(2)–Cl(4) <td>100.05(13)</td> <th>N(3)–Mn(1)–Cl(2)</th> <td>107.44(4)</td> <th>P(1)–Fe(1)–Cl(2)</th> <td>99.10(7)</td> </th></th>	95.28(10)	N(3)–Fe(1)–Cl(2) <td>103.79(12)</td> <th>N(6)–Fe(2)–Cl(4) <td>100.05(13)</td> <th>N(3)–Mn(1)–Cl(2)</th> <td>107.44(4)</td> <th>P(1)–Fe(1)–Cl(2)</th> <td>99.10(7)</td> </th>	103.79(12)	N(6)–Fe(2)–Cl(4) <td>100.05(13)</td> <th>N(3)–Mn(1)–Cl(2)</th> <td>107.44(4)</td> <th>P(1)–Fe(1)–Cl(2)</th> <td>99.10(7)</td>	100.05(13)	N(3)–Mn(1)–Cl(2)	107.44(4)	P(1)–Fe(1)–Cl(2)	99.10(7)
		105.96(4)	C(1)–Fe(1)–Cl(2)	112.16(6)	112.16(6)	Cl(3)–Fe(2)–Cl(4) <td>106.33(8)</td> <th>C(1)–Fe(1)–Cl(2) <td>118.94(6)</td> <th>Cl(3)–Fe(2)–Cl(4) <td>123.09(8)</td> <th>Cl(1)–Mn(1)–Cl(2)</th> <td>112.70(2)</td> <th>Cl(1)–Fe(1)–Cl(2)</th> <td>111.98(8)</td> </th></th>	106.33(8)	C(1)–Fe(1)–Cl(2) <td>118.94(6)</td> <th>Cl(3)–Fe(2)–Cl(4) <td>123.09(8)</td> <th>Cl(1)–Mn(1)–Cl(2)</th> <td>112.70(2)</td> <th>Cl(1)–Fe(1)–Cl(2)</th> <td>111.98(8)</td> </th>	118.94(6)	Cl(3)–Fe(2)–Cl(4) <td>123.09(8)</td> <th>Cl(1)–Mn(1)–Cl(2)</th> <td>112.70(2)</td> <th>Cl(1)–Fe(1)–Cl(2)</th> <td>111.98(8)</td>	123.09(8)	Cl(1)–Mn(1)–Cl(2)	112.70(2)	Cl(1)–Fe(1)–Cl(2)	111.98(8)

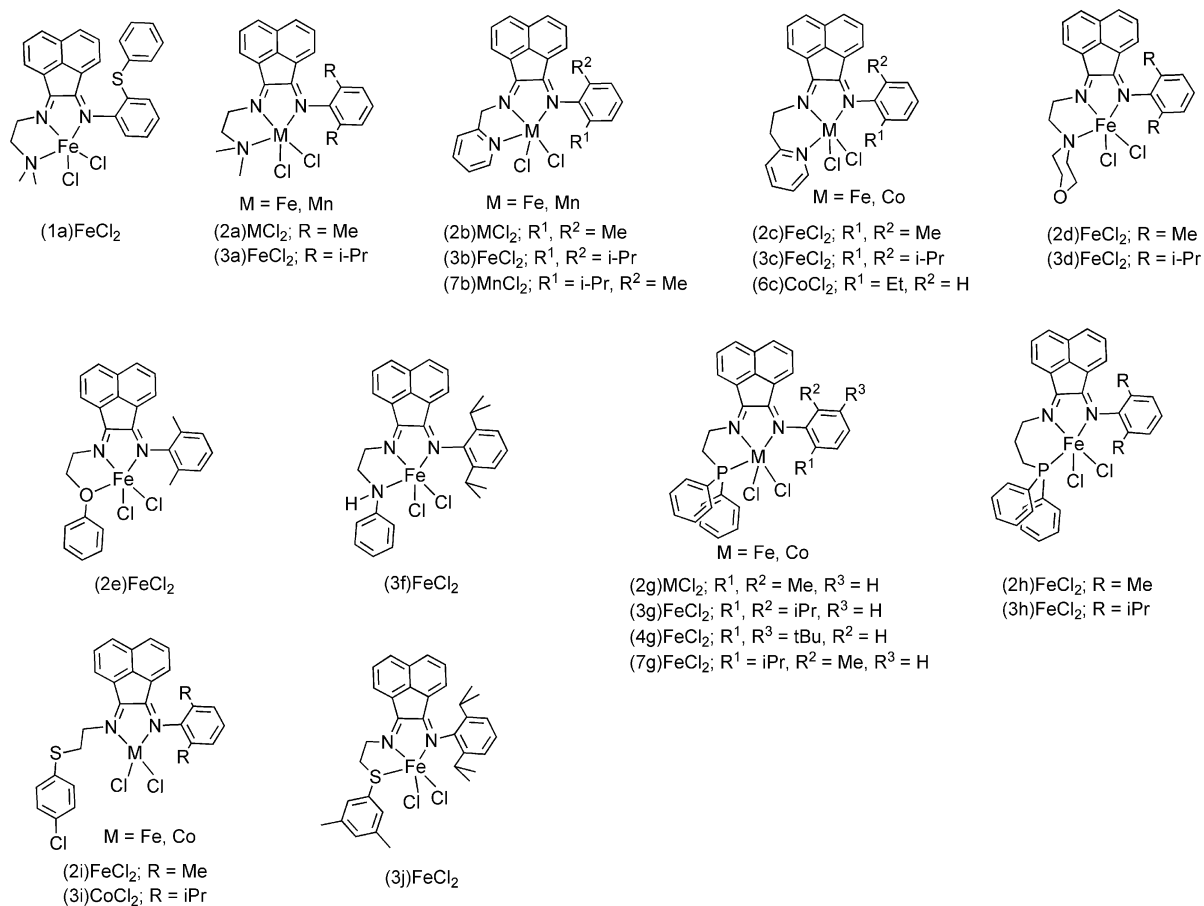
¹H and ¹³C NMR spectroscopy and elemental analysis. Monoimines **2–7** encompass a range of aryl ring substituents and were prepared with the expectation that, as in the case of Ni-diimine^{1,2} and Fe–PBI^{3,4} catalysts, the aryl substitution pattern would have a significant impact on catalytic performance.

With monoimines **2–7** in hand, we turned our attention to the preparation of asymmetric diimine ligands by reaction of the remaining carbonyl group with a donor-modified primary amine. The acenaphthene backbone structure necessarily limited us to pendant donors linked *via* short alkyl spacers as these spacers would minimize unfavorable steric interactions, such as those observed in **1**, between the linking group and the acenaphthenediimine backbone system. Unfortunately, numerous attempts to prepare pure donor-modified α -diimine ligands were unsuccessful. Our efforts were thwarted by the tendency of the (inherently more basic) donor-modified alkylamine to react at the imine and carbonyl groups in **2–7**. While NMR data were consistent with formation of some of the desired donor-modified α -diimine, examination of the reaction mixtures invariably revealed substantial quantities of the free substituted aniline, indicating that reaction was also occurring at the imino group. Furthermore, attempts to isolate and purify the desired donor-modified α -diimine by column chromatography (silica) were unsuccessful due to decomposition (confirmed by ¹H NMR spectroscopy) of the imines back to acenaphthenequinone, a reaction apparently facilitated by the relatively acidic silica chromatographic media. We have not extensively explored the use of other chromatographic supports to purify the α -diimine ligands. Instead we turned our attention to an *in-situ* technique to prepare the α -diimine ligand in the presence of the metal halide, leading to the desired metal complex in one step.

In-situ synthesis of metal complexes supported by donor modified α -diimine ligands

Due to the difficulties in obtaining pure samples of pendant donor-modified α -diimine ligands, we explored a synthetic route that avoids ligand isolation and purification, and instead produces the donor-modified ligand and the metal complex in one step. Utilizing this strategy, shown in Scheme 5, we have prepared

**Scheme 5**



Scheme 6

a fairly extensive family of metal complexes utilizing α -diimine ligands modified with N, O, P and S pendant donor atoms. It is unclear whether the metal halide facilitates ligand formation or whether the metal simply sequesters the ligand once it forms. In any event, crystallization of the metal complex out of the reaction mixture undoubtedly serves to drive formation of the desired metal complex. In a representative synthetic example, treatment of one equivalent of 2,6-methyl substituted monoimine **2** in dry butanol with one equivalent each of *N,N*-dimethylethylenediamine (**a**) and anhydrous iron(II) chloride yields, after overnight heating at 60 °C, a dark green microcrystalline solid of complex (2a)FeCl₂ in 80% yield. Subsequent filtration and drying provided analytically pure material. Similar synthetic procedures have been used to produce the array of metal complexes shown in Scheme 6.

Similar to metal-PBI complexes, the metal complexes in Scheme 6 display magnetic moments consistent with high spin metal centers, and, when sufficiently soluble, possess paramagnetically shifted ¹H NMR spectra. Unfortunately, low compound solubility precluded obtaining reliable NMR spectra for all compounds. In addition, the inherent asymmetry of these molecules, coupled with the broad, and sometimes overlapping resonances, complicated the signal assignments. For these reasons, detailed chemical shift assignments are not provided. However, the observed resonances are useful for compound identification and, when possible, the chemical shifts are included in the Experimental section. Metal complexes have been characterized

by FT-IR and UV-visible spectroscopies, elemental analysis, and magnetic susceptibility; data for each compound can be found in the Experimental section.

Solid state structures

To better understand the nature of metal–ligand binding, we determined the X-ray crystal structures of several derivatives. We were especially interested in the detailed coordination geometry of the metal complex and the extent of metal–pendant donor interactions. X-Ray crystallographic data for (3a)FeCl₂, (2c)FeCl₂, (2d)FeCl₂, (2a)MnCl₂, and (3g)FeCl₂ are presented in Table 1; important distances and angles for these compounds are collected in Table 2. In all cases, the metal complexes adopt 5-coordinate geometries, which can be described as distorted square pyramidal or trigonal bipyramidal structures depending on the pendant donor and the imino-aryl substituents. For all structurally characterized complexes, the formal C=N double bond character of the imino groups is preserved, as evidenced by C=N bond lengths in the range from 1.266(7) Å to 1.304(9) Å.

Complexes supported by tridentate NNN ligands

Crystals suitable for X-ray crystallography were grown by slow cooling or slow evaporation of acetonitrile solutions of the respective compounds. The molecular structures of iron complexes (3a)FeCl₂, (2c)FeCl₂, (2d)FeCl₂ and manganese complex

(2a)MnCl₂ are shown in Fig. 2–5, respectively. Each compound is square pyramidal, with varying degrees of distortion towards trigonal bipyramidal geometry. In the square pyramidal description, the three nitrogen atoms and one chlorine atom reside in the basal plane with the other chlorine occupying the apical position. The square pyramidal descriptions are supported by values of the shape-defining parameter, τ , which are less than 0.43 in all cases, $\tau = 1.0$ describes a perfectly trigonal bipyramidal structure.^{17,18} The four basal atoms are coplanar to within 0.126 Å for (3a)FeCl₂, 0.026 Å and 0.085 Å for (2c)FeCl₂ (two independent molecules), and 0.110 Å for (2a)MnCl₂. For each complex, the metal atom is raised out of the plane by 0.53 Å, 0.58 Å and 0.56 Å (two independent molecules), and 0.73 Å, respectively. For (2d)FeCl₂, deviations from the mean plane are more significant (max. deviation = 0.833 and 0.417 Å for the two independent molecules), with Fe raised out of this plane by 0.523 and 0.648 Å, respectively. Among these four NNN complexes, (2d)FeCl₂ can also be described as a distorted trigonal bipyramid, with N(1), Cl(1) and Cl(2) occupying the trigonal plane and N(2) and N(3) positioned in the axial positions. In such a depiction, the Fe atom resides nearly in the plane formed by N(1), N(2), and N(3) and this plane almost perfectly bisects the Cl–Fe–Cl angle.

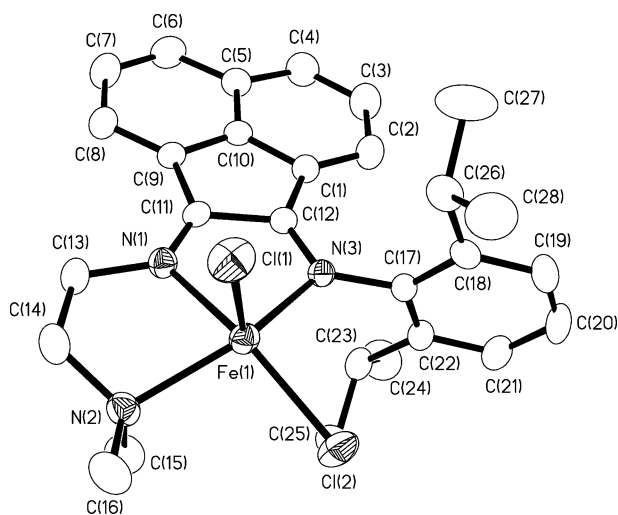


Fig. 2 Thermal ellipsoid representation (35% probability boundaries) of the X-ray crystal structure of (3a)FeCl₂ with hydrogen atoms omitted for clarity.

Complexes with NNN ligation share features in common with structurally characterized iron(II)–PBI complexes. For example, Fe–PBI complexes typically display shorter distances from Fe to the central pyridyl nitrogen (0.070 Å to 0.162 Å shorter for seven structurally characterized complexes)^{3,4a,5,6} than to either of the imino nitrogens, presumably due to the ligand's enforced *mer* coordination geometry. A similar trend is observed for the new NNN ligated complexes reported here, the Fe–N distance to the central imino nitrogen is shorter (ranging from 0.027 to 0.317 Å shorter) than to either of the other nitrogen donors. Other structural similarities include the tendency of the imino-aryl rings to orient nearly orthogonal to the plane containing the metal and nitrogen atoms. Such an arrangement minimizes steric interactions between aryl substituents and the remainder of the molecule. Furthermore, many PBI-supported complexes

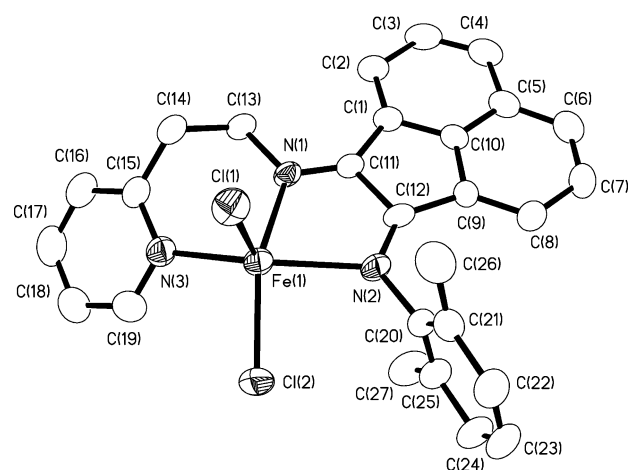


Fig. 3 Thermal ellipsoid representation (35% probability boundaries) of the X-ray crystal structure of (2c)FeCl₂ with hydrogen atoms omitted for clarity.

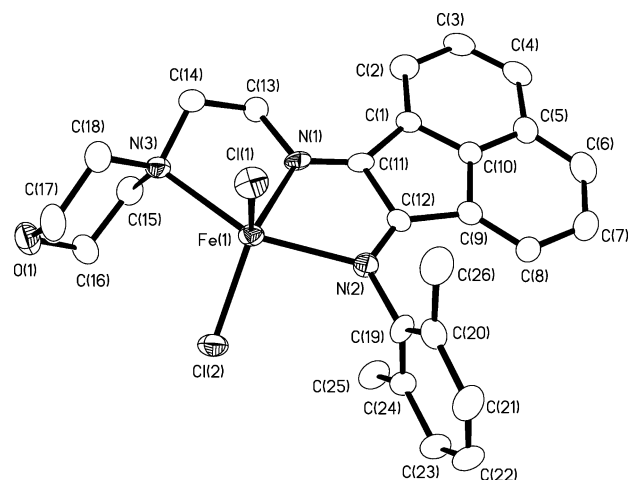


Fig. 4 Thermal ellipsoid representation (35% probability boundaries) of the X-ray crystal structure of (2d)FeCl₂ with hydrogen atoms omitted for clarity.

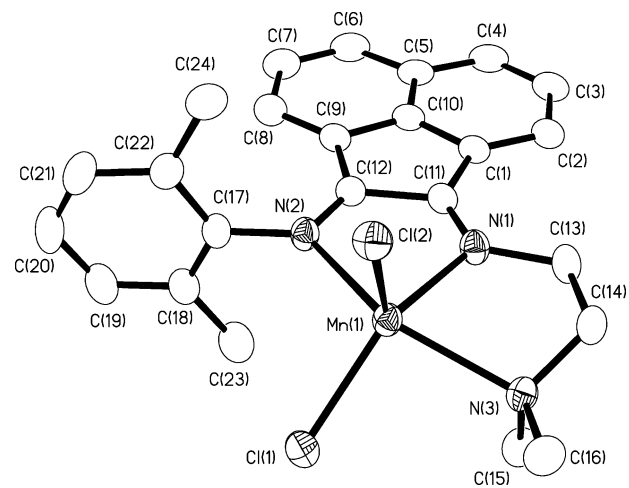


Fig. 5 Thermal ellipsoid representation (35% probability boundaries) of the X-ray crystal structure of (2a)MnCl₂ with hydrogen atoms omitted for clarity.

display elongation along the axial Fe–Cl bond, with this bond typically 0.03 to 0.05 Å longer than its equatorial counterpart. This elongation is also observed in (3a)FeCl₂ and in one of the two molecules in the asymmetric units of both (2c)FeCl₂ and (2d)FeCl₂. However, for (2c)FeCl₂ and (2d)FeCl₂, the second molecule in each asymmetric unit displays slight axial compression, with the axial Fe–Cl bond being 0.016 and 0.014 Å shorter than the respective equatorial bond. The origin of this reversal is unclear as there are no obvious intra- or intermolecular interactions that would cause the observed axial compression.

Complexes (3a)FeCl₂ (Fig. 2) and (2a)MnCl₂ (Fig. 5) provide a direct comparison between Fe(II) and Mn(II) chloride complexes supported by nearly equivalent NNN ligands. As expected, the Mn–N and Mn–Cl distances (Table 2) are slightly longer than the corresponding Fe–N and Fe–Cl distances due to the slightly larger radius of the manganese(II) ion. Other metrical parameters are similar, except that, in (2a)MnCl₂, there is no discernable difference between axial and equatorial Mn–Cl distances (2.3524(5) Å and 2.3495(5) Å), in contrast to the axial elongation noted above for (3a)FeCl₂.

Finally, the morpholine derivative (2d)FeCl₂ possesses a comparatively long Fe–N (pendant donor) bond (2.358(5) Å and 2.356(5) Å for the two independent molecules) relative to the other structurally characterized NNN complexes. The reason for this elongation is unclear as there do not appear to be any obvious interactions between the morpholine ring and the remainder of the molecule.

Complexes supported by tridentate NNP ligands

Crystals of NNP-ligated complex (3g)FeCl₂ were grown by slow evaporation of an acetonitrile solution, which resulted in two acetonitrile molecules in the unit cell. The structure of complex (3g)FeCl₂ is shown in Fig. 6; selected distances and angles can be found in Table 2. The 5-coordinate geometry of (3g)FeCl₂ is adequately described as a distorted square pyramid, with the Fe atom raised 0.606 Å out of the mean basal plane, the maximum deviation of the four basal atoms from their mean plane is 0.18 Å. Consistent with the observed high spin character of (3g)FeCl₂ (*S* = 2, μ_{eff} = 4.7 μ_{B}), the Fe(II)–P distance of 2.497(2) Å is significantly longer than that exhibited by low spin 4-coordinate (square planar) or low-spin 6-coordinate (octahedral)

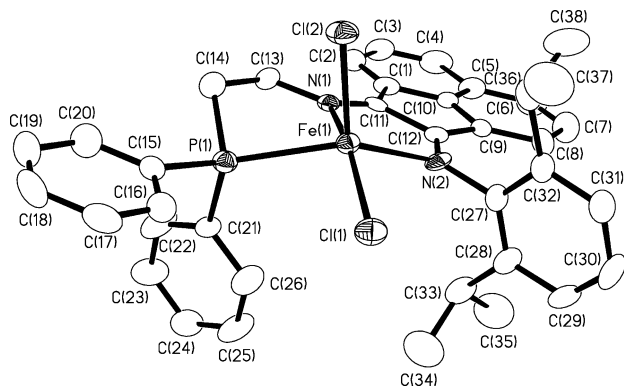


Fig. 6 Thermal ellipsoid representation (35% probability boundaries) of the X-ray crystal structure of (3g)FeCl₂ with hydrogen atoms omitted for clarity.

iron(II)-phosphine complexes (typically 2.23–2.30 Å).^{19,20} Also consistent with its five-coordinate geometry, the Fe(II)–P distance in (3g)FeCl₂ falls between that observed for high spin octahedral (typically 2.58 to 2.71 Å)^{21,22} and tetrahedral (typically 2.41 to 2.47 Å)^{23,24} compounds. As with structurally characterized NNN complexes, (3g)FeCl₂ displays axial Fe–Cl elongation, with the axial bond being 0.026 Å longer than its equatorial counterpart. However, in contrast to NNN ligated complexes, the distance from Fe to the central imino nitrogen (2.181(6) Å) is not statistically different from that to the adjacent imino nitrogen (2.166(6) Å). The relatively long Fe–P bond apparently allows the central imino nitrogen to pull back slightly, resulting in nearly equivalent Fe–N(imino) distances.

Complexes supported by tridentate NNS ligands

Complexes supported by α -diimine ligands with pendant thioether donors (NNS ligands) display far more variety in their coordination geometries. *In-situ* reactions between monoimine ligand **1**, FeCl₂ and several bulky aniline derivatives failed to produce isolable metal complexes. However, when **1** was combined with one equivalent of FeCl₂ and *N,N*-dimethylethylenediamine, complex (1a)FeCl₂ was isolated. A crystal suitable for X-ray crystallography was grown by diffusing pentane into a concentrated dichloromethane solution. X-Ray data collection parameters are given in Table 3 and selected distances and angles are provided in Table 4. The molecular structure of (1a)FeCl₂ is shown in Fig. 7, which clearly shows the presence of a dangling thioether group and a firmly bound *N,N*-dimethylamine donor. The bonding parameters of (1a)FeCl₂ are very similar to those of (3a)FeCl₂ (Fig. 2 and Table 2), including a short Fe–N bond to the central imino nitrogen (2.090(6) Å) and slight elongation of the axial Fe–Cl bond. Thus, the external thioether substituent causes only minor perturbations to the now familiar square pyramidal NNN structure. The inability of sulfur to bind to iron in (1a)FeCl₂ is likely due to the unfavorable steric interactions noted previously between aryl and acenaphthene groups, but may also be due to inherently poor coordinating ability of a thioether sulfur. In order to probe this latter possibility, thioethers linked by alkyl spacers to the acenaphthenediimine backbone are required. The necessary thioether

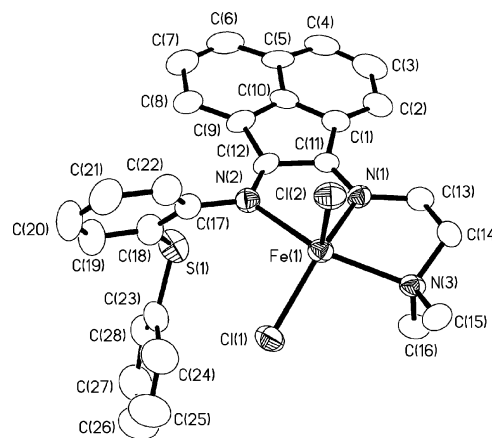


Fig. 7 Thermal ellipsoid representation (35% probability boundaries) of the X-ray crystal structure of (1a)FeCl₂ with hydrogen atoms omitted for clarity.

Table 3 Summary of X-ray crystallographic data for NNS-ligated metal complexes^a

Complex	(1a)FeCl ₂	(2i)FeCl ₂ (MeCN)·1.5 MeCN	[(2i)FeCl ₂] ₂ ·CH ₂ Cl ₂	(3j)FeCl ₂ ·0.5 THF
Empirical formula	C ₂₆ H ₂₅ Cl ₂ FeN ₃ S	C ₃₃ H _{30.50} Cl ₃ FeN _{4.50} S	C ₃₀ H ₂₅ Cl ₃ FeN ₂ S	C ₃₆ H ₄₀ Cl ₂ FeN ₂ O _{0.50} S
FW	562.32	684.38	666.67	667.51
crystal system	Trigonal (rhombohedral)	Monoclinic	Triclinic	Monoclinic
space group	R $\bar{3}$ (hexagonal axes)	P2 ₁ /n	P $\bar{1}$	P2 ₁ /c
a/Å	38.587(6)	10.464(2)	10.095(1)	11.8801(13)
b/Å	38.587(6)	25.493(3)	13.842(1)	17.027(2)
c/Å	10.062(2)	12.312(2)	20.837(3)	16.671(2)
a/Å	90	90	92.33(2)	90
β/Å	90	95.58(2)	92.33(1)	92.91(2)
γ/Å	120	90	92.78(2)	90
V/Å ³	12975(4)	3268.8(9)	2903.2(5)	3367.9(7)
Z	18	4	4	4
d _{calcd} /Mg m ⁻³	1.295	1.391	1.525	1.316
Crystal size/mm	0.40 × 0.20 × 0.10	0.42 × 0.40 × 0.36	0.42 × 0.18 × 0.03	0.30 × 0.22 × 0.20
Abs. Coeff./mm ⁻¹	0.801	0.801	1.075	0.697
2θ max/°	51.96	53.94	50.94	49.42
Transmission range	0.9242–0.7400	0.7615–0.7297	1.0–0.7815	1.000–0.8197
No. of reflns collected	5914	7488	12 053	6026
No. of indep reflns	5649	7106	11 373	5731
No. of obsd reflections	2587	4077	6848	4239
No. of variables	316	399	689	412
R1 (wR2) ^b [I > 2σ(I)]	0.0820 (0.2008)	0.0741 (0.1331)	0.0665 (0.1442)	0.0438 (0.0957)
Goodness-of-fit (F ²)	1.007	1.005	1.008	1.016
Diff. Peaks/e ⁻ Å ⁻³	0.696, -0.479	0.458, -0.855	1.057, -0.778	0.373, -0.324

^a See Experimental section for additional data collection, reduction, and structure solution and refinement details. ^b $R1 = \sum \|F_o\| - |F_c| / \sum \|F_o\|$; $wR2 = [\sum [w(F_o^2 - F_c^2)^2]]^{1/2}$ where $w = 1/\sigma^2(F_o^2) + (aP)^2 + bP$.

amine precursors, 2-(4-chlorophenylthio)ethylamine and 2-(3,5-dimethylphenylthio)ethylamine, are readily prepared by reaction of 2-bromoethylamine hydrobromide with the appropriate thiol in the presence of excess K₂CO₃.²⁵ Distillation of the crude oils (under vacuum) provided thioether amines that were judged to be pure by GC-MS as well as ¹H and ¹³C NMR spectroscopic data. *In-situ* reactions, as outlined in Scheme 5, using these thioether amines provided the sulfur containing metal complexes diagrammed in Scheme 6. Three derivatives were found to be acceptable for X-ray crystallographic analysis: (2i)FeCl₂(MeCN), [(2i)FeCl₂]₂, and (3j)FeCl₂. Data collection parameters are contained in Table 3 and important distances and angles are presented in Table 4. Crystals of complex (2i)FeCl₂(MeCN) were grown by slow evaporation of an acetonitrile solution, giving rise to the solid state structure shown in Fig. 8, with the α-diimine ligand bound in a bidentate fashion and acetonitrile occupying the fifth coordination site at iron. Thus, the strong σ-donating acetonitrile effectively blocks sulfur from coordinating to iron (the Fe–S distance in (2i)FeCl₂(MeCN) is >5.6 Å). Also of note, with the compound freed from the constraints imposed by a tridentate ligand arrangement, (2i)FeCl₂(MeCN) adopts a pseudo-trigonal bipyramidal structure ($\tau = 0.91$) with nearly identical Fe–Cl bond lengths (2.3058(15) and 2.3161(14) Å).

We reasoned that crystallization of (2i)FeCl₂ from a poorly coordinating solvent might allow sulfur ligation; crystallization of (2i)FeCl₂ from dichloromethane (*via* pentane diffusion) provided X-ray quality crystals. However, rather than the hoped for sulfur-ligated compound, the solid state structure, shown in Fig. 9, is that of a chloride-bridged dimer, [(2i)FeCl₂]₂. Thus, at least in the solid state, chloride is a more effective donor to iron than the thioether sulfur atom. Although sulfur does not coordinate to iron in the solid state, we cannot rule out the presence of weak

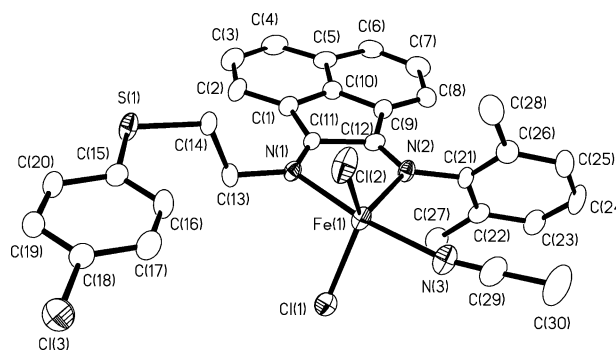
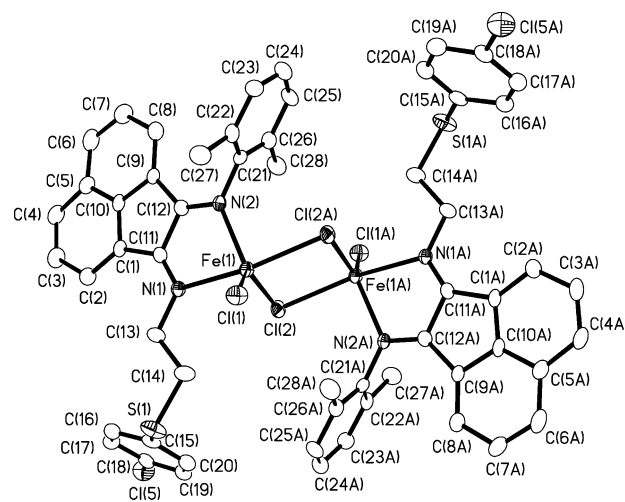
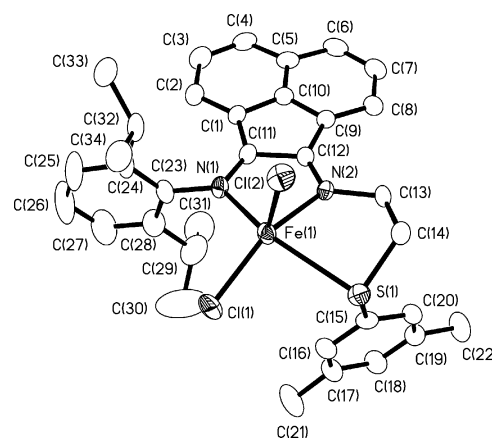


Fig. 8 Thermal ellipsoid representation (35% probability boundaries) of the X-ray crystal structure of (2i)FeCl₂(MeCN) with hydrogen atoms omitted for clarity.

Fe–S interactions when (2i)FeCl₂ is dissolved in non-coordinating solvents. We considered that the 4-chlorophenyl substituent might withdraw electron density from sulfur and contribute to weak sulfur ligation, and that aryl substituents with electron donating groups might enhance the nucleophilicity of sulfur. To test this hypothesis, we prepared the 3,5-dimethylphenyl substituted thioether and used it to synthesize metal complex (3j)FeCl₂. When crystallized from tetrahydrofuran (pentane diffusion), crystals suitable for X-ray diffraction were obtained. The molecular structure of (3j)FeCl₂, shown in Fig. 10, indeed shows a monomeric square pyramidal complex, with a long Fe–S bond of 2.7126(10) Å as compared to other structurally characterized iron–thioether complexes. A search of the Cambridge Structural Database (November 2005 release)²⁶ reveals 271 compounds containing iron–thioether bonds—the majority of these being iron(II) complexes. This collection has a mean Fe–S bond length of

Table 4 Selected distances (Å) and angles (°) for NNS-ligated metal complexes

(1a)FeCl ₂	(2i)FeCl ₂ (MeCN)	(2i)FeCl ₂	Molecule 2	(3j)FeCl ₂
Fe(1)–N(1)	2.090(6)	2.196(4)	Fe(2)–N(3)	2.223(4)
Fe(1)–N(2)	2.215(6)	2.131(4)	Fe(2)–N(4)	2.119(4)
Fe(1)–N(3)	2.219(6)	2.260(2)	Fe(2)–Cl(5)	2.2477(17)
Fe(1)–Cl(1)	2.273(2)	2.3058(15)	Fe(2)–Cl(4)	2.3548(16)
Fe(1)–Cl(2)	2.299(2)	2.3161(14)	Fe(2)–Cl(4a)	2.5367(15)
N(1)–C(11)	1.281(9)	1.269(7)	N(3)–C(41)	1.261(7)
N(2)–C(12)	1.298(9)	1.270(6)	N(4)–C(42)	1.284(7)
N(1)–Fe(1)–N(2)	75.6(2)	78.17(17)	N(3)–Fe(2)–N(4)	77.61(16)
N(1)–Fe(1)–N(3)	75.5(2)	99.85(13)	N(1)–Fe(1)–S(1)	144.24(7)
N(2)–Fe(1)–N(3)	149.0(2)	85.88(13)	N(2)–Fe(1)–S(1)	75.24(7)
N(1)–Fe(1)–Cl(1)	143.45(18)	162.30(12)	N(1)–Fe(1)–Cl(1)	98.92(7)
N(1)–Fe(1)–Cl(2)	103.65(17)	119.98(13)	N(1)–Fe(1)–Cl(2)	106.88(7)
N(2)–Fe(1)–Cl(1)	96.26(17)	110.58(13)	N(2)–Fe(1)–Cl(1)	150.56(7)
N(2)–Fe(1)–Cl(2)	97.71(17)	90.68(13)	N(2)–Fe(1)–Cl(2)	91.60(7)
N(3)–Fe(1)–Cl(1)	99.72(17)	192.26(7)	S(1)–Fe(1)–Cl(1)	93.28(3)
N(3)–Fe(1)–Cl(2)	100.30(16)	97.62(6)	S(1)–Fe(1)–Cl(2)	96.97(3)
Cl(1)–Fe(1)–Cl(2)	112.80(9)	85.25(6)	Cl(1)–Fe(1)–Cl(2)	116.96(4)

Fig. 9 Thermal ellipsoid representation (35% probability boundaries) of the X-ray crystal structure of [(2i)FeCl₂]₂ with hydrogen atoms omitted for clarity.Fig. 10 Thermal ellipsoid representation (35% probability boundaries) of the X-ray crystal structure of (3j)FeCl₂ with hydrogen atoms omitted for clarity.

2.300 Å (min 2.141 Å, max 2.806 Å) and only two complexes in the database have longer Fe–S bonds than that in (3j)FeCl₂. One, an iron(II) compound supported by a PBI-based dithia macrocycle, {[2,15-dimethyl-7,10-dithia-3,14,20-triazabicyclo[14.3.1]eicosa-1(20),2,14,16,18-pentaene-*N,N',N'',S*]}FeCl(MeOH)}ClO₄, possesses the longest Fe–S bond observed to date (2.806 Å).²⁷ The second, {[*N,N'*-bis(2-(2-mercaptophenylthio)ethyl)piperazine]Fe}, ligated by a piperazine-based thiolate–thioether ligand system, displays 2.755 Å Fe–S(thioether) linkages.²⁸ Thus, the Fe–S bond in (3j)FeCl₂ is unusually long and is indicative of a relatively weak Fe–S interaction. We presume that acetonitrile would ligate to iron, analogous to (2i)FeCl₂(MeCN), if (3j)FeCl₂ were recrystallized from this solvent.

The successful isolation of (3j)FeCl₂ suggests that other monomeric, sulfur-bound complexes would form with appropriately chosen alkyl- or aryl-substituted thioethers. We are continuing to examine aryl- and alkylthioether derivatives to further tune the nucleophilicity of sulfur and to better understand the role of Fe–S ligation in ethylene oligomerization reactions catalyzed by iron complexes. This work will be the subject of future

reports. In the meantime, we have discovered that soft donors (like P and S) have a large impact on the catalytic performance of these metal complexes, both in terms of activity and oligomer product properties. Our initial ethylene polymerization results in this area are described in detail elsewhere.²⁹

Summary

We have prepared five-coordinate metal(II) halide complexes supported by a new family of donor-modified α -diimine ligands. Compounds with NNN, NNO, NNP and NNS ligands have been prepared and selected examples of NNN, NNP and NNS derivatives have been structurally characterized by X-ray crystallography. All isolated metal complexes possess high spin electronic configurations. Whereas the structurally characterized NNN and NNP complexes invariably display square pyramidal coordination geometries, NNS-ligated complexes exhibit a range of coordination behaviors (from dimeric, to solvent-ligated, to weakly sulfur-ligated) depending on the crystallization solvent and the apparent nucleophilicity of the thioether sulfur atom.

Experimental

General considerations

Unless otherwise stated, all operations were carried out under argon in a glovebox or using standard Schlenk techniques. Tetrahydrofuran, diethylether, dichloromethane, acetonitrile and pentane were purified by standard drying procedures and stored over activated molecular sieves prior to use. Other reagents were obtained commercially from Aldrich Chemical Company or Acros Organics and used as received. Atlantic Microlab, Inc. (Norcross, GA) performed elemental analyses. Proton and NMR spectra were obtained using either JEOL Eclipse or Bruker AVANCE II 400 MHz spectrometers operating at room temperature. GC-MS spectra were obtained using electron impact (EI) on an HP 5890 gas chromatograph coupled to an HP 5970 mass selective detector. Magnetic susceptibilities were determined at room temperature using a Johnson Matthey magnetic susceptibility balance. Electronic absorption spectra were recorded on a Hewlett-Packard 8453 diode array spectrophotometer (190–1100 nm range). Samples for IR were dispersed in KBr and spectra were recorded on a Nicolet 5DXC spectrometer with a diffuse reflectance (DRIFTS) attachment.

Synthesis of 2-(thioether)ethylamines

2-(4-Chlorophenylthio)ethylamine. To a stirring mixture of 4.07 g (20.0 mmol) of 2-bromoethylamine hydrobromide and 6.00 g (43.4 mmol) of K_2CO_3 in 30 mL of CH_2Cl_2 was added 2.89 g (20.0 mmol) of 4-chlorobenzenethiol. The mixture was stirred at room temperature under argon for 2 d. The mixture was washed twice with distilled water, dried with $MgSO_4$ and filtered. Volatiles were removed *in vacuo* leaving a slightly cloudy yellow oil. Distillation of the oil under reduced pressure (0.10 Torr) at 80–100 °C produced 1.99 g (54.7%) of a clear liquid which was identified as the desired product by its 1H and ^{13}C NMR spectra. 1H NMR (400 MHz, $CDCl_3$): δ = 7.25 (4 H, m), 2.97 (2 H, t), 2.89 (2 H, t), 1.28 (2 H, br s). $^{13}C\{^1H\}$ NMR (100 MHz, $CDCl_3$): δ =

134.32, 132.28, 131.07, 129.08, 40.84, 38.29. EI mass spectrum, m/z 187 [M^+].

2-(3,5-Dimethylphenylthio)ethylamine. To a stirring mixture of 1.93 g (9.4 mmol) of 2-bromoethylamine hydrobromide and 3.00 g (21.7 mmol) of K_2CO_3 in 30 mL of CH_2Cl_2 was added 1.00 g (7.2 mmol) of 3,5-dimethylbenzenethiol. The mixture was stirred at room temperature under argon for 2 d. The mixture was washed twice with distilled water, dried with $MgSO_4$ and filtered. Volatiles were removed *in vacuo* leaving a slightly cloudy yellow oil. Distillation of the oil under reduced pressure (0.10 Torr) at 80–95 °C produced 0.547 g (41.7%) of a clear liquid which was identified as the desired product by its 1H and ^{13}C NMR spectra. 1H NMR (400 MHz, $CDCl_3$): δ = 6.98 (2 H, s), 6.82 (1 H, s), 2.98 (2 H, t), 2.89 (2 H, t), 2.27 (6 H, s), 1.55 (2 H, br s). $^{13}C\{^1H\}$ NMR (100 MHz, $CDCl_3$): δ = 138.58, 135.10, 128.21, 127.50, 41.00, 38.07, 21.29. EI mass spectrum, m/z 181 [M^+].

Synthesis of mono-imine ligands

(E)-2-(2-(Phenylthio)phenylimino)acenaphthylen-1(2H)-one (1). An ethanol (200 mL) solution of acenaphthenequinone (10.0 g, 54.9 mmol) was treated with 1 mL of formic acid, followed by slow, dropwise addition (over approx. 8 h) of a solution of 2-(phenylthio)aniline (11.0 g, 54.9 mmol) in 120 mL of ethanol. The resulting mixture was stirred at 60 °C overnight, cooled to room temperature and filtered to remove unreacted acenaphthenequinone. The filtrate was cooled to –10 °C overnight. The red–orange solid that deposited was filtered, washed with ether and dried to yield 6.68 g (33.3%) of product. The room temperature 1H NMR spectrum appears to be a superposition of spectra (approx. 10 : 1 ratio), perhaps resulting from conformers that interconvert slowly on the NMR timescale due to hindered rotation about the imino aryl substituent. The following NMR data correspond to the predominant isomer. 1H NMR (400 MHz, $CDCl_3$): δ = 8.14 (2 H, t), 7.98 (1 H, d), 7.79 (1 H, t), 7.43–7.18 (5 H, m), 7.03–6.8 (4 H, m), 6.91 (2 H, d). $^{13}C\{^1H\}$ NMR (100 MHz, $CDCl_3$): δ = 189.29, 160.10, 150.32, 143.20, 134.74, 132.41, 132.10, 131.28, 130.93, 130.62, 129.55, 128.95, 128.87, 128.27, 128.09, 127.95, 127.17, 125.90, 125.78, 123.40, 122.12, 118.27. Anal. Calc. (Found) for $C_{24}H_{15}NOS$: C, 78.88 (78.47); H, 4.14 (4.10); N, 3.83 (3.83). EI mass spectrum, m/z 365 [M^+]. Single crystal X-ray crystallography confirmed the monoimine structure.

(2E)-2-[(2,6-Dimethylphenyl)imino]acenaphthylen-1(2H)-one (2). An ethanol (200 mL) solution of acenaphthenequinone (10.0 g, 55 mmol) was treated with 0.5 mL of formic acid, followed by slow, dropwise addition (over approx. 12 h) of a solution of 2,6 dimethylaniline (6.8 mL, 55 mmol) in 60 mL of ethanol. The resulting mixture was stirred at 60 °C overnight, cooled to room temperature and filtered. The filtrate was cooled to 0 °C. After 3 d, the orange solid that deposited was filtered, washed with cold methanol and dried, yielding 4.91 g of pure product. Slow evaporation of the remaining filtrate yielded an additional 5.87 g of orange solid for a total yield of 10.78 g (69%). 1H NMR (400 MHz, $CDCl_3$): δ = 8.18 (2 H, d), 8.00 (1 H, d), 7.82 (1 H, t), 7.43 (1 H, t), 7.15–7.05 (3 H, m), 6.70 (1 H, d), 2.04 (6 H, s). $^{13}C\{^1H\}$ NMR (100 MHz, $CDCl_3$): δ = 189.64, 160.07, 148.51, 142.95, 132.11, 130.97, 130.91, 129.41, 128.49, 128.32, 128.28, 127.74, 124.60,

124.33, 122.53, 122.19, 17.89. Anal. Calc. (Found) for $C_{20}H_{15}NO$: C, 84.19 (83.61); H, 5.30 (5.52); N, 4.91 (5.20). EI mass spectrum, m/z 285 [M^+].

(2E)-2-[(2,6-Diisopropylphenyl)imino]acenaphthylen-1(2H)-one (3). An ethanol (65 mL) solution of acenaphthenequinone (2.0 g, 11 mmol) was treated with 1 mL of formic acid, followed by slow, dropwise addition (over approx. 8 h) of a solution of 2,6-diisopropylaniline (1.6 mL, 8.3 mmol) in 65 mL of ethanol. The resulting mixture was stirred at 60 °C overnight, cooled and filtered. After removal of solvent under vacuum, the resulting orange solid was dissolved in ether, filtered and cooled to -10 °C overnight. The orange solid that deposited was filtered, washed with cold ether and dried. The filtrate was again cooled to -10 °C overnight and more orange solid was isolated, giving a total yield of 1.91 g (68.5%). 1H NMR (400 MHz, $CDCl_3$): δ = 8.18 (2 H, m), 7.99 (1 H, d), 7.81 (1 H, t), 7.39 (1 H, t), 7.25 (3 H, m), 6.62 (1 H, d), 2.82 (2 H, m), 1.16 (6 H, d), 0.88 (6 H, d). 1H NMR (400 MHz, $MeCN-d_3$): δ = 8.27 (1 H, d), 8.12 (2 H, m), 7.87 (1 H, t), 7.45 (1 H, t), 7.30 (3 H, m), 6.60 (1 H, d), 2.79 (2 H, septet), 1.10 (6 H, d), 0.89 (6 H, d). $^{13}C\{^1H\}$ NMR (100 MHz, $CDCl_3$): δ = 189.67, 160.54, 146.53, 143.11, 135.30, 132.23, 131.07, 130.94, 129.41, 128.34, 128.17, 127.70, 125.06, 123.56, 123.39, 122.28, 28.43, 23.47. Anal. Calc. (Found) for $C_{24}H_{23}NO$: C, 84.42 (84.34); H, 6.79 (6.81); N, 4.10 (4.41). EI mass spectrum, m/z 341 [M^+].

(2E)-2-[(2,5-Di-*t*-butylphenyl)imino]acenaphthylen-1(2H)-one (4). An ethanol (65 mL) solution of acenaphthenequinone (2.00 g, 11.0 mmol) was treated with 1 mL of formic acid, followed by slow, dropwise addition (over approx. 8 h) of a solution of 2,5-di-*t*-butylaniline (1.69 g, 8.25 mmol) in 65 mL of ethanol. The resulting mixture was stirred at 60 °C overnight, cooled and filtered to remove unreacted acenaphthenequinone. After removal of solvent under vacuum, the resulting orange solid was dissolved in ether, filtered and cooled to -10 °C overnight. The orange solid that deposited was filtered, washed with cold ether and dried. The filtrate was again cooled to -10 °C overnight and additional product was isolated, giving a total yield of 2.13 g (70%). 1H NMR (400 MHz, $CDCl_3$): δ = 1.24 (9 H, s), 1.31 (9 H, s), 6.80 (1 H, d), 6.88 (1 H, d), 7.23 (1 H, d), 7.40 (1 H, t), 7.44 (1 H, d), 7.81 (1 H, t), 7.97 (1 H, d), 8.17 (2 H, d). $^{13}C\{^1H\}$ NMR (100 MHz, $CDCl_3$): δ = 189.78, 158.33, 149.41, 149.24, 143.43, 136.93, 132.03, 131.09, 130.86, 129.03, 128.79, 128.16, 127.82, 126.59, 123.62, 122.07, 121.85, 115.98, 35.03, 34.43, 31.19, 29.87. Anal. Calc. (Found) for $C_{26}H_{27}NO$: C, 84.51 (84.48); H, 7.37 (7.46); N, 3.79 (3.82). EI mass spectrum, m/z 369 [M^+].

(E)-2-(2-*t*-Butylphenylimino)acenaphthylen-1(2H)-one (5). An ethanol (80 mL) solution of acenaphthenequinone (2.00 g, 11.0 mmol) was treated with 1 mL of formic acid, followed by dropwise addition (over approx. 5 h) of a solution of 2-*t*-butylaniline (1.3 mL, 8.3 mmol) in 50 mL of ethanol. The resulting mixture was stirred at 60 °C overnight. Unreacted acenaphthenequinone was removed by filtration and the filtrate was evaporated to dryness. The orange residue was dissolved in diethylether and filtered. The resulting solution was reduced in volume to the saturation point and cooled to -10 °C overnight, yielding 0.588 g (22.7%) of orange solid. 1H NMR analysis showed it to be a 15 : 1 mixture of monoimine : diimine; recrystallization from diethylether did not significantly alter this ratio. 1H NMR

(400 MHz, $CDCl_3$): δ = 8.17 (2 H, d), 7.98 (1 H, d), 7.81 (1 H, t), 7.53 (1 H, d), 7.42 (1 H, t), 7.22 (2 H, m), 6.85 (1 H, d), 6.77 (1 H, d), 1.32 (9 H, s). $^{13}C\{^1H\}$ NMR (100 MHz, $CDCl_3$): δ = 189.66, 158.42, 149.69, 143.46, 139.70, 132.06, 131.06, 130.81, 129.06, 128.19, 127.97, 126.92, 126.63, 126.34, 125.37, 123.80, 122.11, 118.25, 35.46, 29.82. Anal. Calc. (Found) for $C_{22}H_{19}NO$: C, 84.31 (83.82); H, 6.11 (6.32); N, 4.47 (4.46). EI mass spectrum, m/z 313 [M^+].

(E)-2-(2-Ethylphenylimino)acenaphthylen-1(2H)-one (6). An ethanol (70 mL) solution of acenaphthenequinone (2.00 g, 11.0 mmol) was treated with 1 mL of formic acid, followed by dropwise addition (over approx. 5 h) of a solution of 2-ethylaniline (1.0 mL, 8.3 mmol) in 70 mL of ethanol. The resulting orange mixture was stirred at 60 °C overnight. Unreacted acenaphthenequinone was removed by filtration and the filtrate was cooled to -10 °C overnight, yielding 0.100 g of orange solid. Further concentration of the filtrate and cooling to -10 °C deposited an additional 0.652 g of orange product, giving a total yield of 0.752 g (31.9%). 1H NMR (400 MHz, $CDCl_3$): δ = 8.17 (2 H, d), 7.99 (1 H, d), 7.82 (1 H, t), 7.42 (1 H, t), 7.36 (1 H, m), 7.25 (2 H, m), 6.87 (1 H, m), 6.84 (1 H, d), 2.54 (2 H, q), 1.05 (3 H, t). $^{13}C\{^1H\}$ NMR (100 MHz, $CDCl_3$): δ = 189.69, 159.44, 149.14, 143.36, 132.80, 132.12, 131.04, 130.79, 129.23, 129.07, 128.24, 128.06, 127.22, 126.58, 125.36, 123.49, 122.20, 117.00, 24.57, 14.38. Anal. Calc. (Found) for $C_{20}H_{15}NO$: C, 84.19 (83.73); H, 5.30 (5.35); N, 4.91 (4.91). EI mass spectrum, m/z 285 [M^+].

(E)-2-(2-Isopropyl-6-methylphenylimino)acenaphthylen-1(2H)-one (7). An ethanol (50 mL) solution of acenaphthenequinone (2.00 g, 11.0 mmol) was treated with 1 mL of formic acid, followed by dropwise addition (over approx. 5 h) of a solution of 2-isopropyl-6-methylaniline (1.3 mL, 8.3 mmol) in 70 mL of ethanol. The resulting orange mixture was stirred at 60 °C overnight. Unreacted acenaphthenequinone was removed by filtration and solvent was removed *in vacuo*. The orange residue was dissolved in diethylether, filtered and reduced in volume until incipient crystallization. Cooling this solution to -10 °C overnight deposited 0.594 g of orange solid. Further concentration of the filtrate and cooling to -10 °C deposited an additional 0.094 g of orange product, giving a total yield of 0.684 g (26.5%). 1H NMR (400 MHz, $CDCl_3$): δ = 8.18 (2 H, d), 7.99 (1 H, d), 7.82 (1 H, t), 7.42 (1 H, t), 7.26 (1 H, d), 7.18-7.12 (2 H, m), 6.67 (1 H, d), 2.92 (1 H, septet), 2.00 (3 H, s), 1.20 (3 H, d), 0.89 (3H, s). $^{13}C\{^1H\}$ NMR (100 MHz, $CDCl_3$): δ = 189.61, 160.32, 147.42, 143.00, 136.00, 132.13, 131.00, 130.90, 129.38, 128.37, 128.28, 128.15, 127.78, 124.70, 124.04, 123.68, 122.80, 122.20, 28.48, 23.79, 22.89, 18.07. Anal. Calc. (Found) for $C_{22}H_{19}NO$: C, 84.31 (83.81); H, 6.11 (6.14); N, 4.47 (4.40). EI mass spectrum, m/z 313 [M^+].

Synthesis of metal complexes

[(1a)FeCl₂]. A solution containing 0.10 mL (0.91 mmol) of *N,N*-dimethylethylenediamine in 50 mL of anhydrous butanol was added (*via* cannula) to 0.333 g (0.91 mmol) of **1** and 0.115 g (0.91 mmol) of FeCl₂. The initial orange color changed to green and, after stirring overnight under argon at 55 °C, a black-green solid deposited, which was filtered, washed with 4 mL of THF, and dried to yield 0.411 g (80.3%) of grey-green product. 1H NMR

(400 MHz, MeCN- d_3): δ = 29.66, 25.56, 25.39, 24.74, 20.57, 18.69, 7.01, 6.44, 6.28, -0.69, -7.92. FTIR (KBr): 2899, 2876, 1573, 1457, 1288, 1024, 827, 778, 734 cm^{-1} . UV-vis (CH_3CN) [λ_{max} , nm (ϵ , $\text{M}^{-1} \text{cm}^{-1}$)] 796 (3600). Anal. Calc. (Found) for $\text{C}_{28}\text{H}_{25}\text{N}_3\text{SCl}_2\text{Fe}$: C, 59.81 (60.32); H, 4.48 (4.74); N, 7.47 (7.20). $\mu_{\text{eff}} = 4.7 \mu_{\text{B}}$.

[(2a)FeCl₂]. A solution containing 0.10 mL (0.91 mmol) of *N,N*-dimethylethylenediamine in 50 mL of anhydrous butanol was added (*via* cannula) to 0.260 g (0.91 mmol) of **2** and 0.115 g (0.91 mmol) of FeCl₂. The initially orange solution turned dark green within 20 min and deposited a microcrystalline solid after stirring overnight under argon at 55 °C. The solid was filtered, washed with 6 mL of THF, and dried to yield 0.354 g (80.7%) of dark green product. ¹H NMR (400 MHz, MeCN- d_3): δ = 26.18, 26.01, 20.88, 19.44, 16.35, 6.1, 5.44, 2.50, -0.93, -5.60. FTIR (KBr): 2904, 1643, 1463, 1287, 1025, 915, 827, 783, 762 cm^{-1} . UV-vis (CH_3CN) [λ_{max} , nm (ϵ , $\text{M}^{-1} \text{cm}^{-1}$)] 776 (3860). Anal. Calc. (Found) for $\text{C}_{24}\text{H}_{25}\text{N}_3\text{Cl}_2\text{Fe}$: C, 59.78 (59.80); H, 5.23 (5.29); N, 8.71 (8.72). $\mu_{\text{eff}} = 4.9 \mu_{\text{B}}$.

[(2a)MnCl₂]. A solution containing 0.10 mL (0.91 mmol) of *N,N*-dimethylethylenediamine in 50 mL of anhydrous butanol was added (*via* cannula) to 0.260 g (0.91 mmol) of **2** and 0.115 g (0.91 mmol) of MnCl₂. After overnight heating under argon at 55 °C, a tan solid precipitated. This solid was filtered, washed with 6 mL of toluene, and dried to yield 0.324 g (74.0%) of brown product. The sample was not sufficiently soluble in acetonitrile for NMR analysis. FTIR (KBr): 2888, 1693, 1649, 1594, 1468, 932, 844, 794, 773 cm^{-1} . UV-vis (CH_3CN) spectroscopy did not reveal any prominent transitions in the visible region. We were unable to obtain satisfactory carbon analysis on this manganese derivative, however an X-ray crystal structure determination confirmed its formulation as the tridentate complex. Anal. Calc. (Found) for $\text{C}_{24}\text{H}_{25}\text{N}_3\text{Cl}_2\text{Mn}$: C, 59.89 (54.37); H, 5.24 (5.19); N, 8.73 (8.81). $\mu_{\text{eff}} = 5.5 \mu_{\text{B}}$.

[(2b)FeCl₂]. A solution containing 0.10 mL (1.0 mmol) of 2-(aminomethyl)pyridine in 50 mL of anhydrous butanol was added (*via* cannula) to 0.285 g (1.0 mmol) of **2** and 0.127 g (1.0 mmol) of FeCl₂. The initially orange solution turned dark brown within 20 min and deposited a dark solid after stirring overnight under argon at 55 °C. The solid was filtered, washed with 6 mL of THF, and dried to yield 0.242 g (48.2%) of product. The sample was not sufficiently soluble in acetonitrile for reliable NMR characterization. FTIR (KBr): 3058, 2954, 2913, 1646, 1605, 1466, 1286, 829, 767 cm^{-1} . UV-vis (CH_3CN) [λ_{max} , nm (ϵ , $\text{M}^{-1} \text{cm}^{-1}$)] 504 (1500). This compound analyzed consistently low for carbon. Anal. Calc. (Found) for $\text{C}_{26}\text{H}_{21}\text{N}_3\text{Cl}_2\text{Fe}$: C, 62.18 (59.17); H, 4.21 (4.07); N, 8.37 (8.77). $\mu_{\text{eff}} = 4.6 \mu_{\text{B}}$.

[(2b)MnCl₂]. A solution containing 0.16 mL (1.6 mmol) of 2-(aminomethyl)pyridine in 50 mL of anhydrous butanol was added (*via* cannula) to 0.450 g (1.58 mmol) of **2** and 0.198 g (1.58 mmol) of MnCl₂. After overnight heating under argon at 55 °C, a brown solid precipitated. This solid was filtered, washed with 6 mL of THF, and dried to yield 0.450 g (56.8%) of brown product. The sample was not sufficiently soluble in acetonitrile for NMR analysis. FTIR (KBr): 3058, 2920, 1688, 1646, 1591, 1473, 1438, 1362, 1293, 1044, 836, 781 cm^{-1} . UV-vis (CH_3CN) spectroscopy

did not reveal any discernable transition in the visible region. Anal. Calc. (Found) for $\text{C}_{26}\text{H}_{21}\text{N}_3\text{Cl}_2\text{Mn}$: C, 62.29 (62.15); H, 4.22 (4.60); N, 8.38 (7.91). $\mu_{\text{eff}} = 5.1 \mu_{\text{B}}$.

[(2c)FeCl₂]. A solution containing 0.11 mL (0.91 mmol) of 2-(aminoethyl)pyridine in 50 mL of anhydrous butanol was added (*via* cannula) to 0.260 g (0.91 mmol) of **2** and 0.115 g (0.91 mmol) of FeCl₂. The initially orange solution turned dark green and deposited a green solid within 2 h. After stirring overnight under argon at 55 °C the solid was filtered, washed with 6 mL of THF, and dried to yield 0.269 g (57.2%) of green product. ¹H NMR (400 MHz, MeCN- d_3): δ = 44.2, 22.72, 20.0, 18.14, 17.50, 16.32, 15.86, 3.75, 2.96, 2.8, -2.72. FTIR (KBr): 2953, 2904, 1655, 1594, 1484, 1441, 1282, 1046, 832, 773 cm^{-1} . UV-vis (CH_3CN) [λ_{max} , nm (ϵ , $\text{M}^{-1} \text{cm}^{-1}$)] 730 (2500). Anal. Calc. (Found) for $\text{C}_{27}\text{H}_{23}\text{N}_3\text{Cl}_2\text{Fe}$: C, 62.82 (62.58); H, 4.49 (4.42); N, 8.14 (8.13). $\mu_{\text{eff}} = 5.7 \mu_{\text{B}}$.

[(2d)FeCl₂]. A solution containing 0.10 mL (0.76 mmol) of 4-(2-aminoethyl)morpholine in 50 mL of anhydrous butanol was added (*via* cannula) to 0.217 g (0.76 mmol) of **2** and 0.096 g (0.76 mmol) of FeCl₂. Within 2 h, green solid precipitated out of solution. After stirring overnight under argon at 55 °C, the solid was filtered, washed with 4 mL of THF, and dried to yield 0.283 g (71.0%) of green solid. ¹H NMR (400 MHz, MeCN- d_3): δ = 26.02, 18.13, 17.76, 17.50, 6.04, 5.49, 5.16, 4.34, 3.40, -1.71. FTIR (KBr): 2959, 2915, 2871, 1671, 1600, 1277, 1118, 1041, 915, 832, 773 cm^{-1} . UV-vis (CH_3CN) [λ_{max} , nm (ϵ , $\text{M}^{-1} \text{cm}^{-1}$)] 736 (2200). Anal. Calc. (Found) for $\text{C}_{26}\text{H}_{27}\text{N}_3\text{OCl}_2\text{Fe}$: C, 59.57 (59.59); H, 5.19 (5.16); N, 8.01 (7.93).

[(2e)FeCl₂]. A solution containing 0.10 mL (0.77 mmol) 2-phenoxyethylamine in 50 mL of anhydrous butanol was added (*via* cannula) to 0.220 g (0.77 mmol) of **2** and 0.098 g (0.77 mmol) of FeCl₂. Immediately upon addition the solution became a dark green. After stirring overnight under argon at 55 °C, a green colored solid was filtered, washed with 4 mL of THF, and dried to yield 0.144 g (35.1%) of green product. ¹H NMR (400 MHz, MeCN- d_3): δ = 12.06, 10.17, 8.63, 7.20, 6.78, 5.73, 5.20, -0.36, -5.78, -11.93. FTIR (KBr): 3038, 2920, 1598, 1501, 1245, 1051, 781, 698 cm^{-1} . UV-vis (CH_3CN) [λ_{max} , nm (ϵ , $\text{M}^{-1} \text{cm}^{-1}$)] 648 (430). Anal. Calc. (Found) for $\text{C}_{28}\text{H}_{24}\text{N}_2\text{OCl}_2\text{Fe}$: C, 63.30 (63.49); H, 4.55 (4.55); N, 5.27 (5.36).

[(2g)FeCl₂]. A solution of 0.211 g (0.92 mmol) of 2-(diphenylphosphino)ethylamine in 40 mL of anhydrous butanol was added *via* cannula to 0.263 g (0.92 mmol) of **2** and 0.117 g (0.92 mmol) of anhydrous FeCl₂. The solution was stirred overnight under argon at 55 °C. The solid that formed was filtered, washed with a small amount of THF, and dried to give 0.380 g (66%) of dark green product. ¹H NMR (400 MHz, MeCN- d_3): δ = 39.7, 16.44, 14.15, 13.74, 12.9, 12.5, 8.0, 7.43, 7.1, 6.2, 5.5, -1.42, -6.3. FTIR (KBr): 2953, 2910, 1655, 1605, 1490, 1441, 838, 789, 739, 701 cm^{-1} . UV-vis (CH_3CN) [λ_{max} , nm (ϵ , $\text{M}^{-1} \text{cm}^{-1}$)] 752 (1300). Anal. Calc. (Found) for $\text{C}_{34}\text{H}_{29}\text{N}_2\text{P}_2\text{Cl}_2\text{Fe}$: C, 65.51 (65.07); H, 4.69 (4.68); N, 4.49 (4.49). $\mu_{\text{eff}} = 5.0 \mu_{\text{B}}$.

[(2g)CoCl₂]. A solution containing 0.242 g (1.05 mmol) 2-(diphenylphosphino)ethylamine in 40 mL of anhydrous butanol was added (*via* cannula) to 0.301 g (0.96 mmol) of **2** and 0.137 g (1.05 mmol) of CoCl₂. After stirring overnight under argon at

55 °C, the solution was cooled and the resulting solid was filtered, washed with diethylether, and dried to yield 0.363 g (55.1%) of rusty-brown product. The sample was not sufficiently soluble in acetonitrile for NMR analysis. FTIR (KBr): 2910, 1666, 1627, 1584, 1484, 1436, 838, 778, 740, 696 cm⁻¹. UV-vis spectroscopy did not reveal any discernable transition in the visible region. Anal. Calc. (Found) for C₃₄H₂₉N₂PCl₂Co: C, 65.19 (64.49); H, 4.67 (4.73); N, 4.47 (4.41). $\mu_{\text{eff}} = 4.4 \mu_{\text{B}}$.

[(2h)FeCl₂]. A solution containing 0.229 g (0.94 mmol) 3-(diphenylphosphino)-1-propylamine in 50 mL of anhydrous butanol was added (*via* cannula) to 0.268 g (0.94 mmol) of **2** and 0.119 g (0.94 mmol) of FeCl₂. After stirring overnight under argon at 55 °C, the solution was reduced in volume to 10 mL and the resulting solid was filtered, washed with 4 mL of THF, and dried to yield 0.406 g (67.7%) of aqua-colored product. The compound was not sufficiently soluble in acetonitrile for reliable NMR characterization. FTIR (KBr): 2950, 1642, 1594, 1474, 1436, 832, 789, 745, 701 cm⁻¹. UV-vis (CH₃CN) [λ_{max} , nm (ϵ , M⁻¹ cm⁻¹)] 714 (1100). This compound analyzed as the monohydrate. Anal. Calc. (Found) for C₃₅H₃₃N₂OPCl₂Fe: C, 64.14 (63.02); H, 5.07 (4.90); N, 4.27 (3.91); O, 2.44 (2.99).

[(2i)FeCl₂]. A solution containing 0.202 g (0.928 mmol) of 2-(4-chlorophenylthio)ethylamine in 10 mL of anhydrous butanol was added (*via* cannula) to 0.265 g (0.928 mmol) of **2** and 0.118 g (0.928 mmol) of FeCl₂ in 40 mL of anhydrous butanol. The initially orange solution turned dark green and deposited a green solid within 2 h. After overnight stirring under argon at 55 °C, the green solid was filtered, washed with 6 mL of THF, and dried to yield 0.203 g (37.5%) of product. ¹H NMR (400 MHz, MeCN-d₃): $\delta = 11.79, 11.39, 9.93, 9.50, 7.24, 4.88, -3.03, -11.80$. FTIR (KBr): 2939, 2915, 1665, 1633, 1584, 1479, 1101, 833, 811, 789, 773 cm⁻¹. UV-vis (CH₃CN) [λ_{max} , nm (ϵ , M⁻¹ cm⁻¹)] 656 (340). Anal. Calc. (Found) for C₅₆H₄₆N₄S₂Cl₆Fe₂: C, 57.80 (57.58); H, 3.98 (4.03); N, 4.82 (4.68). $\mu_{\text{eff}} = 4.4 \mu_{\text{B}}$ per Fe.

[(3a)FeCl₂]. A solution containing 0.10 mL (0.91 mmol) of *N,N*-dimethylethylenediamine in 75 mL of anhydrous butanol was added (*via* cannula) to 0.310 g (0.91 mmol) of **3** and 0.115 g (0.91 mmol) of FeCl₂. The initially orange solution turned dark green within 20 min and deposited a microcrystalline solid after stirring overnight under argon at 55 °C. The solid was filtered, washed with 6 mL of THF, and dried to yield 0.327 g (66.7%) of dark green product. ¹H NMR (400 MHz, MeCN-d₃): $\delta = 26.51, 25.15, 24.19, 21.25, 19.86, 7.27, -1.42, -3.62, -5.34$. FTIR (KBr): 2959, 2915, 2849, 1649, 1441, 1287, 1145, 827, 778 cm⁻¹. UV-vis (CH₃CN) [λ_{max} , nm (ϵ , M⁻¹ cm⁻¹)] 784 (4000). Anal. Calc. (Found) for C₂₈H₃₃N₃Cl₂Fe: C, 62.47 (62.36); H, 6.18 (6.20); N, 7.81 (7.83). $\mu_{\text{eff}} = 4.9 \mu_{\text{B}}$.

[(3b)FeCl₂]. A solution containing 0.10 mL (1 mmol) of 2-(aminomethyl)pyridine in 50 mL of anhydrous butanol was added (*via* cannula) to 0.342 g (0.91 mmol) of **3** and 0.127 g (1 mmol) of FeCl₂. The initially orange solution turned dark green within 20 min and deposited a dark green solid after stirring overnight under argon at 55 °C. The solid was filtered, washed with 6 mL of THF, and dried to yield 0.449 g (80%) of dark green product. The sample was not sufficiently soluble in acetonitrile for reliable NMR characterization. FTIR (KBr): 2959, 2920, 2860, 1643, 1594, 1298, 1046, 778 cm⁻¹. UV-vis (CH₃CN) [λ_{max} , nm (ϵ , M⁻¹ cm⁻¹)]

808 (2000). This compound analyzed satisfactorily as the THF monosolvate. Anal. Calc. (Found) for C₃₄H₃₇N₃OCl₂Fe: C, 64.78 (64.48); H, 5.92 (6.09); N, 6.67 (6.61). $\mu_{\text{eff}} = 5.0 \mu_{\text{B}}$.

[(3c)FeCl₂]. A solution containing 0.11 mL (0.91 mmol) of 2-(aminoethyl)pyridine in 50 mL of anhydrous butanol was added (*via* cannula) to 0.310 g (0.91 mmol) of **3** and 0.115 g (0.91 mmol) of FeCl₂. The initially orange solution turned dark brown and deposited a green solid after stirring overnight under argon at 55 °C. The solid was filtered, washed with 6 mL of THF, and dried to yield 0.290 g (55.7%) of green microcrystalline product. ¹H NMR (400 MHz, MeCN-d₃): $\delta = 45.5, 26.25, 21.70, 21.0, 18.10, 5.85, 5.50, 3.46, 3.00, -1.38, -3.23$. FTIR (KBr): 2920, 1653, 1598, 1438, 1313, 1182, 829, 766 cm⁻¹. UV-vis (CH₃CN) [λ_{max} , nm (ϵ , M⁻¹ cm⁻¹)] 720 (2400). Anal. Calc. (Found) for C₃₁H₃₁N₃Cl₂Fe: C, 65.05 (64.81); H, 5.46 (5.55); N, 7.34 (7.30). $\mu_{\text{eff}} = 5.3 \mu_{\text{B}}$.

[(3d)FeCl₂]. A solution containing 0.10 mL (0.76 mmol) 4-(2-aminoethyl)morpholine in 50 mL of anhydrous butanol was added (*via* cannula) to 0.260 g (0.76 mmol) of **3** and 0.096 g (0.76 mmol) of FeCl₂. The initial orange color changed to green and, after stirring overnight under argon at 55 °C, a green solid deposited, which was filtered, washed with 4 mL of THF, and dried to yield 0.267 g (60.4%) of green product. ¹H NMR (400 MHz, MeCN-d₃): $\delta = 24.47, 17.2, 15.72, 10.2, 7.76, 4.97, 3.64, -1.19, -2.28$. FTIR (KBr): 2948, 2858, 1666, 1598, 1459, 1293, 1113, 829, 781 cm⁻¹. UV-vis (CH₃CN) [λ_{max} , nm (ϵ , M⁻¹ cm⁻¹)] 738 (1900). This compound analyzed satisfactorily with 1.5 H₂O per metal complex. Anal. Calc. (Found) for C₃₀H₃₈N₃O_{2.5}Cl₂Fe: C, 59.32 (59.27); H, 6.30 (6.26); N, 6.92 (6.48). $\mu_{\text{eff}} = 5.0 \mu_{\text{B}}$.

[(3f)FeCl₂]. A solution containing 0.10 mL (0.79 mmol) of *N*-phenylethylenediamine in 50 mL of anhydrous butanol was added (*via* cannula) to 0.269 g (0.79 mmol) of **3** and 0.100 g (0.79 mmol) of FeCl₂. After overnight heating under argon at 55 °C, a dark microcrystalline solid precipitated. This solid was filtered, washed with 6 mL of THF, and dried to yield 0.153 g (32.9%) of product. ¹H NMR (400 MHz, MeCN-d₃): $\delta = 15.79, 10.04, 9.5, 9.0, 6.3, 5.3, 2.99, -0.62, -6.0, -7.4$. FTIR (KBr): 2968, 2864, 1598, 1486, 1286, 1210, 946, 829, 781 cm⁻¹. UV-vis (CH₃CN) [λ_{max} , nm (ϵ , M⁻¹ cm⁻¹)] 758 (890). Anal. Calc. (Found) for C₃₂H₃₃N₃Cl₂Fe: C, 65.55 (64.69); H, 5.67 (5.64); N, 7.17 (7.05). $\mu_{\text{eff}} = 4.8 \mu_{\text{B}}$.

[(3g)FeCl₂]. A solution containing 0.297 g (1.29 mmol) 2-(diphenylphosphino)ethylamine in 50 mL of anhydrous butanol was added (*via* cannula) to 0.44 g (1.29 mmol) of **3** and 0.164 g (1.29 mmol) of FeCl₂. After stirring overnight under argon at 55 °C, a microcrystalline solid was filtered, washed with 4 mL of THF, and dried to yield 0.505 g (57.6%) of aqua-colored product. ¹H NMR (400 MHz, MeCN-d₃): $\delta = 21.5, 15.86, 12.80, 6.68, 4.21, 0.52, -1.41, -2.15, -6.5$. FTIR (KBr): 2959, 2860, 1643, 1594, 1430, 1293, 1041, 832, 773, 690 cm⁻¹. UV-vis (CH₃CN) [λ_{max} , nm (ϵ , M⁻¹ cm⁻¹)] 754 (1600). This compound analyzed satisfactorily as the monohydrate. Anal. Calc. (Found) for C₃₈H₃₉N₂OPCl₂Fe: C, 65.44 (65.92); H, 5.64 (5.82); N, 4.02 (3.72). $\mu_{\text{eff}} = 4.7 \mu_{\text{B}}$.

[(3h)FeCl₂]. A solution containing 0.276 g (1.13 mmol) 3-(diphenylphosphino)-1-propylamine in 50 mL of anhydrous butanol was added (*via* cannula) to 0.387 g (1.13 mmol) of **3** and 0.144 g (1.13 mmol) of FeCl₂. After stirring overnight under argon

at 55 °C, a dark green solid precipitated. This solid was collected, washed with diethylether, and dried to yield 0.577 g (73.7%) of dark green product. ¹H NMR (400 MHz, MeCN-d₃): δ = 26.9, 21.9, 19.1, 17.0, 11.6, 5.8, -1.16, -3.22, -4.71, -7.4. FTIR (KBr): 3052, 2959, 2860, 1643, 1468, 1430, 1288, 788, 734, 701 cm⁻¹. UV-vis (CH₃CN) [λ_{max} , nm (ϵ , M⁻¹ cm⁻¹)] 714 (2400). Anal. Calc. (Found) for C₃₉H₃₉N₂PCl₂Fe: C, 67.55 (67.43); H, 5.67 (6.00); N, 4.04 (3.83). μ_{eff} = 5.2 μ_{B} .

[(3i)CoCl₂]. A solution containing 0.318 g (1.46 mmol) of 2-(4-chlorophenylthio)ethylamine in 10 mL of anhydrous butanol was added (*via* cannula) to 0.501 g (1.46 mmol) of **3** and 0.191 g (1.46 mmol) of CoCl₂ in 40 mL of anhydrous butanol. After stirring overnight under argon at 55 °C, the solution was taken to dryness and the resulting solid was washed with diethylether and dried to yield 0.727 g (79.5%) of dark green product. The sample was not sufficiently soluble in acetonitrile for NMR analysis. FTIR (KBr): 2970, 1632, 1589, 1485, 1299, 1096, 1014, 838, 778 cm⁻¹. UV-vis (CH₃CN) [λ_{max} , nm (ϵ , M⁻¹ cm⁻¹)] 672 (390). This compound is presumably the chloride-bridged dimer, by analogy to iron derivative [(2i)FeCl₂]. Anal. Calc. (Found) for C₆₄H₆₂N₄S₂Cl₆Co₂: C, 59.96 (59.54); H, 4.88 (4.91); N, 4.37 (4.42). μ_{eff} = 4.4 μ_{B} per Co.

[(3j)FeCl₂]. A solution containing 0.189 g (1.04 mmol) of 2-(3,5-dimethylphenylthio)ethylamine in 50 mL of anhydrous butanol was added (*via* cannula) to 0.356 g (1.04 mmol) of **3** and 0.132 g (1.04 mmol) of FeCl₂. After stirring overnight under argon at 55 °C, volatiles were removed *in vacuo* and the resulting solid was filtered, washed with 6 mL of diethylether, and dried to yield 0.320 g (48.7%) of green-brown product. ¹H NMR (400 MHz, MeCN-d₃): δ = 13.80, 10.71, 10.41, 8.18, 7.28, 4.86, 2.50, -0.16, -9.72. FTIR (KBr): 2766, 2925, 2888, 1582, 1488, 1464, 1286, 1054, 832, 781 cm⁻¹. UV-vis (CH₃CN) [λ_{max} , nm (ϵ , M⁻¹ cm⁻¹)] 444sh (3180). The compound analyzed as the monohydrate. Anal. Calc. (Found) for C₃₄H₃₆N₂SCl₂Fe: C, 62.87 (60.85); H, 5.90 (5.79); N, 4.31 (4.32); O, 2.46 (1.92).

[(4g)FeCl₂]. A solution of 0.235 g (1.02 mmol) of 2-(diphenylphosphino)ethylamine in 10 mL of anhydrous butanol was added *via* cannula to 0.380 g (1.02 mmol) of **4** and 0.130 g (1.02 mmol) of anhydrous FeCl₂ followed by 40 mL of anhydrous butanol. The green solution was stirred overnight under argon at 55 °C and reduced in volume to about 10 mL. The solid that precipitated was filtered, washed with a small amount of diethylether, and dried to give 0.352 g (48.8%) of dark green product. ¹H NMR (400 MHz, MeCN-d₃): δ = 39.7, 16.44, 14.15, 13.74, 12.9, 12.5, 8.0, 7.43, 7.1, 6.2, 5.5, -1.42, -6.3. FTIR (KBr): 2970, 2866, 1611, 1490, 1436, 1293, 838, 784, 745, 707 cm⁻¹. UV-vis (CH₃CN) [λ_{max} , nm (ϵ , M⁻¹ cm⁻¹)] 732 (740). This compound afforded satisfactory elemental analysis as the monohydrate. Anal. Calc. (Found) for C₄₀H₄₃N₂OPCl₂Fe: C, 66.22 (65.80); H, 5.97 (5.77); N, 3.86 (3.60).

[(6c)CoCl₂]. A solution containing 0.10 mL (0.85 mmol) of 2-(aminoethyl)pyridine in 40 mL of anhydrous butanol was added (*via* cannula) to 0.243 g (0.85 mmol) of **6** and 0.110 g (0.85 mmol) of CoCl₂. A dark solid deposited after stirring overnight under argon at 55 °C. The solid was filtered, washed with 6 mL of diethylether, and dried to yield 0.195 g (44.2%) of product. The compound was

not sufficiently soluble in acetonitrile for NMR analysis. FTIR (KBr): 2964, 2936, 2873, 1627, 1604, 1484, 1445, 1296, 1249, 1160, 835, 780, 767 cm⁻¹. UV-vis (CH₃CN) [λ_{max} , nm (ϵ , M⁻¹ cm⁻¹)] 656 (520). Anal. Calc. (Found) for C₂₇H₂₃N₃Cl₂Co: C, 62.44 (62.05); H, 4.46 (4.47); N, 8.09 (8.01). μ_{eff} = 4.3 μ_{B} .

[(7b)MnCl₂]. A solution containing 0.15 mL (1.5 mmol) of 2-(aminomethyl)pyridine in 50 mL of anhydrous butanol was added (*via* cannula) to 0.450 g (1.44 mmol) of **7** and 0.181 g (1.44 mmol) of MnCl₂. After overnight heating under argon at 55 °C, a yellow-orange solid precipitated. This solid was filtered, washed with 6 mL of THF, and dried to yield 0.305 g (56.8%) of product. The sample was not sufficiently soluble in acetonitrile for NMR analysis. FTIR (KBr): 2962, 1673, 1584, 1293, 1051, 1016, 781 cm⁻¹. UV-vis (CH₃CN) spectroscopy did not reveal any prominent transitions in the visible region. Anal. Calc. (Found) for C₂₈H₂₅N₃Cl₂Mn: C, 63.53 (63.34); H, 4.76 (5.09); N, 7.94 (7.55). μ_{eff} = 5.3 μ_{B} .

[(7g)FeCl₂]. A solution containing 0.206 g (0.90 mmol) 2-(diphenylphosphino)ethylamine in 40 mL of anhydrous butanol was added (*via* cannula) to 0.281 g (0.90 mmol) of **7** and 0.114 g (0.90 mmol) of FeCl₂. After stirring overnight under argon at 55 °C, the solution was reduced in volume and filtered. The residue was dissolved in THF, filtered and precipitated by adding diethylether. The solid was collected and dried to yield 0.307 g (52.4%) of dark green product. FTIR (KBr): 2964, 2926, 2866, 1594, 1430, 1145, 838, 784, 696 cm⁻¹. UV-vis (CH₃CN) [λ_{max} , nm (ϵ , M⁻¹ cm⁻¹)] 752 (850). This compound gave satisfactory elemental analysis as the monohydrate. Anal. Calc. (Found) for C₃₆H₃₅N₂OPCl₂Fe: C, 64.59 (64.20); H, 5.27 (5.16); N, 4.18 (3.96); O, 2.39 (2.69).

X-Ray crystallography

Single crystals were mounted in thin-walled glass capillaries and transferred to a Bruker-Nonius MACH3S X-ray diffractometer for data collections at either 25 °C (**1**, complexes (**3a**)FeCl₂, (**2c**)FeCl₂, (**1a**)FeCl₂, (**2i**)FeCl₂(MeCN), and [(**2i**)FeCl₂]₂) or -100 °C (complexes (**2d**)FeCl₂, (**2a**)MnCl₂, (**3g**)FeCl₂, and (**3j**)FeCl₂) using graphite monochromated Mo K α (λ = 0.71073 Å) radiation. Unit cell constants were determined from a least squares refinement of the setting angles of 25 intense, high angle reflections. Intensity data were collected using the $\omega/2\theta$ scan technique to a maximum 2θ value of 50–55°. Absorption corrections were applied based on azimuthal scans of several reflections for each sample as required. The data were corrected for Lorentz and polarization effects and converted to structure factors using the Crystal-Structure software package.³⁰ Space groups were determined based on systematic absences and intensity statistics. Successful direct-methods solutions were calculated for each compound using the SHELXTL suite of programs.³¹ Any non-hydrogen atoms not identified from the initial E-map were located after several cycles of structure expansion and full matrix least squares refinement on F^2 . Hydrogen atoms were added geometrically. All non-hydrogen atoms were refined with anisotropic displacement parameters, while hydrogen atoms were refined using a riding model with group isotropic displacement parameters. Relevant

crystallographic information for the compounds is summarized in Tables 1 and 3.

In complex (**2c**)FeCl₂, the sample was found as expected with two crystallographically independent yet chemically similar complexes occupying the asymmetric unit in addition to a single acetonitrile solvate (resulting in the fractional elemental compositions found in the empirical formula). The sample was robust throughout the majority of the room temperature data collection. However, within the last 2–3 h, the sample experienced significant (<60%) decay due to rapid desolvation. No attempt was made to scale the data for this decay, as the reflections being measured at that time were principally weak, high θ data. However, as a result of the sample decay, azimuthal scan data for a semi-empirical absorption correction could not be collected. Thus, the data for (**2c**)FeCl₂ were not treated for either decay or absorption.

For complex (**2d**)FeCl₂, doubling of the unit cell dimensions yields cell parameters that are close to a C-centered monoclinic cell (with $a = 20.56$ Å, $b = 20.27$ Å, $c = 12.32$ Å, $\alpha = 89.9^\circ$, $\beta = 107.1^\circ$, $\gamma = 90.8^\circ$); however, the Laue symmetry of the data is clearly $\bar{1}$ rather than $2/m$. Moreover, $R(\text{merge})$ for the monoclinic cell is more than 0.6. Assignment of the Laue class as triclinic is supported by the successful solution and refinement of the structure in the triclinic space group $P\bar{1}$. Two independent molecules of (**2d**)FeCl₂ are present in the asymmetric unit, with metrical differences that well exceed the uncertainties in the calculated bond lengths and angles.

In the case of (**1a**)FeCl₂, nearly all of the peaks in the final difference map are located within channels that are arrayed around $\bar{3}$ axes that traverse the unit cell. It is highly likely that fractional, disordered solvent is present within these channels. However, attempts to model this solvent with CH₂Cl₂ or pentane (from which the sample was crystallized) was not successful. The diffuse scattering of the low-occupancy, disordered solvent is responsible for the large residuals reported for this complex. In support of this notion, the SOLV/SQUEEZE utility in the PLATON suite of programs identified a solvent accessible volume of 1484 Å³ in the unit cell (11.4% of total cell volume), occupied by a total disordered electron density of 71 e⁻ per cell.³² This corresponds to approximately two pentane or two CH₂Cl₂ molecules per cell (1/9th of a solvate molecule per molecule of complex per cell). The contributions of these disordered solvate molecules to F_o were removed using the SQUEEZE utility, and refinement converged using the modified structure factors. The contributions of the removed solvate molecules are not included in the final d_{calcd} , F_{000} , or the formula weight of the complex. Data collection for (**1a**)FeCl₂ was not possible at reduced temperature as all of the specimens examined suffered from cracking or splitting at -100 °C, presumably the result of a phase change.

Crystals of (**2i**)FeCl₂(MeCN) were found to be highly solvated. There is one acetonitrile ligand, one fully occupied acetonitrile solvate, and a second, half-occupied acetonitrile solvate that is disordered over an inversion center. Finally, in the case of (**3j**)FeCl₂, a half-occupied molecule of THF was found to be disordered on an inversion center. Refinement of the remaining structures proceeded normally.

CCDC reference numbers 636867–636876.

For crystallographic data in CIF or other electronic format see DOI: 10.1039/b702197f

Acknowledgements

We thank Chevron Phillips Chemical Company for their generous support of this work at the University of Wisconsin-Eau Claire and for permission to publish these results. In addition, we thank the donors of the Petroleum Research Fund, administered by the American Chemical Society (Grant 37885-GB3 to M. J. C.), Research Corporation (Cottrell College Science Award to M. J. C.), the National Science Foundation (CHE-0078746 to J. A. H.) and the University of Wisconsin-Eau Claire for financial support. Instrumentation for infrared analyses (CHE-0216058) and NMR spectroscopic measurements (CHE-0521019) was obtained with the support of the National Science Foundation MRI grant program. We also thank Mr Daniel Bates for assistance in acquiring UV-vis and IR characterization data for this study.

References

- (a) L. K. Johnson, C. M. Killian and M. Brookhart, *J. Am. Chem. Soc.*, 1995, **117**, 6414–6415; (b) C. M. Killian, D. J. Tempel, L. K. Johnson and M. Brookhart, *J. Am. Chem. Soc.*, 1996, **118**, 11664–11665; (c) S. A. Svejda, L. K. Johnson and M. Brookhart, *J. Am. Chem. Soc.*, 1999, **121**, 10634–10635; (d) L. H. Shultz and M. Brookhart, *Organometallics*, 2001, **20**, 3975–3982.
- (a) L. K. Johnson, S. Mecking and M. Brookhart, *J. Am. Chem. Soc.*, 1996, **118**, 267–268; (b) D. J. Tempel, L. K. Johnson, R. L. Huff, P. S. White and M. Brookhart, *J. Am. Chem. Soc.*, 2000, **122**, 6686–6700.
- (a) G. J. P. Britovsek, V. C. Gibson, B. S. Kimberley, P. J. Maddox, S. J. McTavish, G. A. Solan, A. J. P. White and D. J. Williams, *Chem. Commun.*, 1998, 849–850; (b) G. J. P. Britovsek, M. Bruce, V. C. Gibson, B. S. Kimberley, P. J. Maddox, S. Mastroianni, S. J. McTavish, C. Redshaw, G. A. Solan, S. Strömberg, A. J. P. White and D. J. Williams, *J. Am. Chem. Soc.*, 1999, **121**, 8728–8740; (c) G. J. P. Britovsek, S. Mastroianni, G. A. Solan, S. P. D. Baugh, C. Redshaw, V. C. Gibson, A. J. P. White, D. J. Williams and M. R. J. Elsegood, *Chem.–Eur. J.*, 2000, **6**, 2221–2231.
- (a) B. L. Small, M. Brookhart and A. M. A. Bennett, *J. Am. Chem. Soc.*, 1998, **120**, 4049–4050; (b) B. L. Small and M. Brookhart, *J. Am. Chem. Soc.*, 1998, **120**, 7143–7144; (c) A. M. A. Bennett, *Chemtech*, 1999, **29**, 24.
- Y. Chen, R. Chen, C. Qian, X. Dong and J. Sun, *Organometallics*, 2003, **22**, 4312–4321.
- Y. Chen, C. Qian and J. Sun, *Organometallics*, 2003, **22**, 1231–1236.
- M. E. Bluhm, C. Folli and M. Döring, *J. Mol. Catal. A: Chem.*, 2004, **212**, 13–18.
- C. Bianchini, G. Mantovani, A. Meli, F. Migliacci, F. Zanobini, F. Laschi and A. Sommacchi, *Eur. J. Inorg. Chem.*, 2003, 1620–1631.
- C. Bianchini, G. Giambastiani, I. T. Guerrero, A. Meli, E. Passaglia and T. Gragnoli, *Organometallics*, 2004, **23**, 6087–6089.
- W.-H. Sun, X. Tang, T. Gao, B. Wu, W. Zhang and H. Ma, *Organometallics*, 2004, **23**, 5037–5047.
- T. M. Smit, A. K. Tomov, V. C. Gibson, A. J. P. White and D. J. Williams, *Inorg. Chem.*, 2004, **43**, 6511–6512.
- G. J. P. Britovsek, V. C. Gibson, B. S. Kimberley, S. Mastroianni, C. Redshaw, G. A. Solan, A. J. P. White and D. J. Williams, *J. Chem. Soc., Dalton Trans.*, 2001, 1639–1644.
- G. J. P. Britovsek, V. C. Gibson, O. D. Hoarau, S. K. Spitzmesser, A. J. P. White and D. J. Williams, *Inorg. Chem.*, 2003, **42**, 3454–3465.
- M. Gasperini, F. Ragaini, E. Gazzola, A. Caselli and P. Macchi, *Dalton Trans.*, 2004, 3376–3382.
- We have also reported the synthesis of asymmetric PBI ligands and monoimine acetylpyridine (NNO) ligands for use in chromium-based olefin polymerization catalysis. B. L. Small, M. J. Carney, D. M. Holman, C. E. O'Rourke and J. A. Halfen, *Macromolecules*, 2004, **37**, 4375–4386.
- Recently, Ragaini *et al.* postulated that *n*-alkyl imines of acenaphthenequinone are unstable and decompose *via* an isomerization process that releases ring strain in the initially formed alkyimine. The isomerization involves a sp²–sp³ rehybridization of the acenaphthene ring carbon atom, followed by further reaction with another equivalent

- of alkylamine to release an alkyl-imine product. Similar monoimine instability and decomposition processes may account for our inability to isolate monoimines using donor-modified alkylamines. F. Ragaini, M. Gasperini, E. Gallo and P. Macchi, *Chem. Commun.*, 2005, 1031–1033.
- 17 The geometric parameter τ is defined as $\tau = |\beta - a|/60$, where a and β are the two trans basal angles in pseudo-square pyramidal geometry (see ref. 18). In idealized square-planar geometries, $a = \beta$, but trigonal distortions result in $a \neq \beta$.
- 18 A. W. Addison, T. N. Rao, J. van Reedijk, J. Rijn and G. C. Vorscheor, *J. Chem. Soc., Dalton Trans.*, 1984, 1349–1356.
- 19 M. Di Vaira, S. Midollini and L. Sacconi, *Inorg. Chem.*, 1981, **20**, 3430–3435.
- 20 In addition, the Fe(II)–P distances in low spin Fe(η^5 -C₅H₅)-[N(SiMe₂CH₂PPh₂)₂] range from 2.242 to 2.256 Å; M. D. Fryzuk, D. B. Leznoff, E. S. F. Ma, S. J. Rettig and V. G. Young, Jr., *Organometallics*, 1998, **17**, 2313–2323.
- 21 The Fe(II)–P distances in six-coordinate [FeBr₂(PPh₂CH=CHPPh₂)₂] are 2.636 Å and 2.666 Å. R. Ceconi, M. di Vaira and L. Sacconi, *Cryst. Struct. Commun.*, 1981, **10**, 1523. The Fe(II)–P distances in [FeCl₂(PPh₂CH=CHPPh₂)₂] range from 2.576 Å to 2.592 Å; R. Ceconi, M. di Vaira, S. Midollini, A. Orlandini and L. Sacconi, *Inorg. Chem.*, 1981, **20**, 3423.
- 22 The Fe(II)–P distances in six-coordinate [FeCl₂(*o*-(Ph₂P)₂C₆H₄)₂] are 2.612 Å and 2.623 Å; J. E. Barclay, A. Hills, D. L. Hughes and G. J. Leigh, *J. Chem. Soc., Dalton Trans.*, 1988, 2871.
- 23 The Fe(II)–P distances in four-coordinate [FeBr₂(PEt₃)₂] range from 2.406 Å to 2.451 Å; B. S. Snyder and R. H. Holm, *Inorg. Chem.*, 1988, **27**, 2339.
- 24 The Fe(II)–P distances in four-coordinate [Fe(B(CH₂PPh₂)₃)(NH-*p*-C₆H₄Me)] are 2.427 Å and 2.452 Å; S. D. Brown and J. C. Peters, *J. Am. Chem. Soc.*, 2004, **126**, 4538.
- 25 A. R. Katritzky, Y.-J. Hu, H.-Y. He and S. Mehta, *J. Org. Chem.*, 2001, **66**, 5590–5594.
- 26 F. H. Allen, *Acta Crystallogr., Sect. B*, 2002, **B58**, 380–388.
- 27 C. Cairns, S. M. Nelson and M. G. B. Drew, *J. Chem. Soc., Dalton Trans.*, 1981, 1965.
- 28 R. E. Marsh, *Acta Crystallogr., Sect. B: Struct. Sci.*, 2004, **B60**, 252.
- 29 B. L. Small, R. Rios, E. R. Fernandez and M. J. Carney, *Organometallics*, 2007, **26**, 1744–1749.
- 30 *CrystalStructure 3.6.0: Crystal Structure Analysis Package*, Rigaku and Rigaku/MSK 9009, New Trails Dr., The Woodlands, TX 77381 USA, 2000–2004.
- 31 *SHELXTL-NT V. 6.12*, Bruker AXS, Inc., 5465 E. Cheryl Parkway Madison, WI 53711–5373 USA, 2000.
- 32 A. L. Spek, *J. Appl. Crystallogr.*, 2003, **36**, 7–13.